

The Differences Between *Cis*- and *Trans*-Gene Inactivation Caused by Heterochromatin in *Drosophila*

Yuriy A. Abramov,^{*,1} Aleksei S. Shatskikh,^{*,1} Oksana G. Maksimenko,[†] Silvia Bonaccorsi,[‡]

Vladimir A. Gvozdev,^{*,2} and Sergey A. Lavrov^{*,2}

^{*}Department of Molecular Genetics of the Cell, Institute of Molecular Genetics, Russian Academy of Science, Moscow 123182, Russia, and [†]Institute of Gene Biology, Russian Academy of Sciences, 119334 Moscow, Russia, and [‡]Department of Biology and Biotechnology "Charles Darwin," Sapienza University of Rome, 00185, Italy

ABSTRACT Position-effect variegation (PEV) is the epigenetic disruption of gene expression near the *de novo*-formed euchromatin-heterochromatin border. Heterochromatic *cis*-inactivation may be accompanied by the *trans*-inactivation of genes on a normal homologous chromosome in *trans*-heterozygous combination with a PEV-inducing rearrangement. We characterize a new genetic system, inversion *In(2)A4*, demonstrating *cis*-acting PEV as well as *trans*-inactivation of the reporter transgenes on the homologous nonrearranged chromosome. The *cis*-effect of heterochromatin in the inversion results not only in repression but also in activation of genes, and it varies at different developmental stages. While *cis*-actions affect only a few juxtaposed genes, *trans*-inactivation is observed in a 500-kb region and demonstrates a nonuniform pattern of repression with intermingled regions where no transgene repression occurs. There is no repression around the histone gene cluster and in some other euchromatic sites. *trans*-inactivation is accompanied by dragging of euchromatic regions into the heterochromatic compartment, but the histone gene cluster, located in the middle of the *trans*-inactivated region, was shown to be evicted from the heterochromatin. We demonstrate that *trans*-inactivation is followed by *de novo* HP1a accumulation in the affected transgene; *trans*-inactivation is specifically favored by the chromatin remodeler SAYP and prevented by Argonaute AGO2.

KEYWORDS heterochromatin; *Drosophila*; PEV; *trans*-inactivation; nuclear compartmentalization

Position-effect variegation (PEV) is an epigenetic phenomenon of inactivation of a gene in a portion of cells caused by relocation of a gene into or very close to the heterochromatin. Heterochromatin has a distinct chromatin structure that includes specific histone modifications, associated proteins, and a condensed nucleosome package. This structure can spread from the euchromatin-heterochromatic border into the euchromatin by self-assembly and propagation of a complex containing SU(VAR)3-9 histone methyltransferase,

HP1a, and SU(VAR)3-7 proteins, thus affecting the expression of euchromatic genes near the border (Grewal and Elgin 2002; Schotta *et al.* 2003; Hines *et al.* 2009; Elgin and Reuter 2013). Analysis of the spreading of heterochromatin using high-throughput approaches has been performed in a single paper aimed at the analysis of *white-mottled* X-chromosomal inversions, demonstrating PEV of the *white* gene (Vogel *et al.* 2009). It was found that HP1a propagates up to 175 kb into euchromatin from the heterochromatin border and demonstrates uneven distribution over the spreading area. Only the *white* gene among 20 measured genes in this region demonstrates decreased expression as a result of PEV.

Here we present a detailed study of the genetic system (inversion *In(2)A4*) demonstrating *cis*-effects of heterochromatin on gene expression as well as inversion-induced *trans*-inactivation of the transgenes located on the homologous nonrearranged chromosome. RNA-Seq analysis shows that only a few euchromatin genes near the breakpoint of *In(2)A4*

Copyright © 2016 by the Genetics Society of America

doi: 10.1534/genetics.115.181693

Manuscript received August 28, 2015; accepted for publication October 13, 2015; published Early Online October 22, 2015.

Supporting information is available online at www.genetics.org/lookup/suppl/doi:10.1534/genetics.115.181693/-/DC1

NGS data have been submitted to the GEO database at NCBI under accession number GSE71842.

¹These authors contributed equally to this work.

²Corresponding authors: Department of Molecular Genetics of the Cell, Institute of Molecular Genetics, Russian Academy of Sciences, Moscow 123182, Russia. E-mails: gvozdev@img.ras.ru and slavrov@img.ras.ru

significantly change their expression levels, similar to *white-mottled* rearrangements (Vogel *et al.* 2009). We detected not only the repression but also the activation of euchromatic genes as the *cis*-effect of inversion. We also found that *cis*-effects of heterochromatin on a given gene depend on developmental stage. To our knowledge, these peculiar *cis*-effects of heterochromatin on the adjacent euchromatic region have not been reported previously, while the phenomenon of discontinuous heterochromatinization of euchromatic regions near the breakpoint has been discussed (Talbert and Henikoff 2006).

In contrast to relatively weak *cis*-effects, the inversion *In(2)A4* causes strong and widespread inactivation of the *mini-white* reporter in transgenes on homologous nonrearranged chromosomes [preliminary data in Abramov *et al.* (2011)]. Only a few examples of *trans*-action of heterochromatin have been reported to date, and the most extensively studied case of heterochromatin-induced *trans*-inactivation is the *bw^D* allele induced by insertion of a satellite DNA fragment into the coding region of the *brown* gene (Sage *et al.* 2005). Both *In(2)A4* and *bw^D* are able to repress the *mini-white*-containing transgenes on a homologous chromosome by dragging these region into the heterochromatic compartment. Unlike *bw^D*, *In(2)A4* is the inversion causing significant perturbation of chromosome organization. In combination with the wild-type chromosome, it forms a loop as a result of homolog pairing and the sticking together of the separated heterochromatin block and the main pericentromeric heterochromatin. Spatial organization of the loop in the nuclear compartment appears to be the reason for the complex pattern of *trans*-inactivation that includes the noninactivated region of the histone gene cluster.

cis-Effects of heterochromatin on neighbor genes in a rearranged chromosome and *trans*-inactivation of transgenes are considered to be independent processes because the transgene can be inactivated, while a gene at a homologous site on the rearranged *In(2)A4* chromosome may remain either unaffected or even show increased transcription. HP1a accumulation was detected at *trans*-inactivated transgenes, but not on a homologous site on the *In(2)A4* chromosome. We show the proteins specifically affecting *trans*-inactivation: chromatin remodeler SAYP enhances the repression, while the component of the small interfering RNA (siRNA) pathway and possible insulator protein AGO2 prevents it. Our data point to different molecular mechanisms of *cis*-acting PEV and *trans*-inactivation caused by *In(2)A4*.

Materials and Methods

Fly stocks

Strain A12 was created from the *y¹ w^{67c23}* progenitor by introducing the *P*-element-based transgenic construction carrying the *mini-white* and *LacZ* reporter genes (Tulin *et al.* 1998). The transgene is inserted at the beginning of 5' UTR of the *Hr39* gene (position chr2L:21237278). A12 flies have a

uniform red eye color owing to expression of the *mini-white* transgene (Figure 1C). Inversion *In(2)A4* (hereafter A4) was produced by X-ray irradiation of A12 flies and screening of progeny for eye color variegation. A4 is the inversion with the breakpoints in the left arm of chromosome 2 near the transgene position and in the pericentromeric heterochromatin. A4/A4 flies demonstrate variegated eye color (Figure 1C), reduced viability, and female sterility. *In(2)A4(ΔP)* (hereafter A4(ΔP)) is the A4 derivative with the *mini-white* transgene removed by transposase-induced precise excision. A4(ΔP)/A4(ΔP) flies do not contain the reporter genes *mini-white* and *LacZ* but are undistinguishable from A4/A4 in other aspects.

Trans-Inactivation evaluation

The *trans*-inactivating ability of the A4(ΔP) inversion was tested over a set of *mini-white*-containing transgene insertions in the 38D–40F region of chromosome 2 (69 in total, listed in Supporting Information, Table S1). These stocks, carrying different types of transgenes, *i.e.*, *P[lacW]*, *P[EP]*, *P[EPgy2]*, *PBac[RB]*, *PBac[WH]*, *P[GT1]*, *P[wHy]*, *PBac[5HPw(+)]*, and *P[XP]*, were obtained from Bloomington and Szeged collections.

To test the susceptibility of the reporter transgene to *trans*-inactivation, crosses *w^{*}; A4(ΔP)/CyO* females to *w^{*}; P(w)/CyO* males were performed (here and later *P(w)* denotes a normal chromosome bearing the *mini-white* transgene in the 38D–40F region). Eye colors of the *P(w)/A4(ΔP)* and *P(w)/CyO* siblings were compared, and the degree of *trans*-inactivation for each insertion was visually estimated and ranged as no (–), weak (+), medium (++), and strong (+++) inactivation (Figure 1D).

Crosses to check the impact of position-effect modifiers

A number of mutations known to affect chromatin state were tested for their effects on *cis*- and *trans*-inactivation (listed in Table S4). *trans*-Inactivated transgenes 11127 (*P[lacW]*), 20708 (*P[EPgy2]*), and 17134 (*P[EPgy2]*) were taken for this testing and demonstrated similar responses.

To test the effect of the mutation in the gene *e(y)3* (SAYP), located on the X chromosome, the homozygous-viable allele *e(y)3^{u1}* was used (Shidlovskii *et al.* 2005). The *w^{*} e(y)3^{u1}/FM7; A4/CyO* females were crossed to *w^{*}; P(w)/CyO* males. The eye phenotypes of the *w^{*} e(y)3^{u1}/Y; A4/P(w)* and *e(y)3^{u1}/Y; P(w)/CyO* males were compared.

To test the effects of dominant *Su(var)3^{*}* mutations on chromosome 3 (in genes *Su(var)3-9*, *Su(var)3-6*, *Su(var)3-1*, and *Su(var)3-7*) (Table S4 lists the alleles), the crosses of *w^{m4h}/Y; Su(var)3^{*}/TM3, Sb Ser* males to *yw/yw; SM1, CyRoi; TM6b, Tb* females were performed. The F₁ males *yw/Y; SM1, CyRoi; Su(var)3^{*}/TM6b, Tb* were then crossed to females *A4/SM1, CyO; TM3, Sb Ser* to produce F₂ *yw/yw; A4/SM1, CyRoi; Su(var)3^{*}/TM3, Sb Ser* females. These females were crossed to males *yw/Y; P(w)/SM1, CyO*. Eye colors of *yw/Y; A4/P(w); Su(var)3^{*}* and *yw/Y; P(w)/SM1, CyO; Su(var)3^{*}* males were compared.

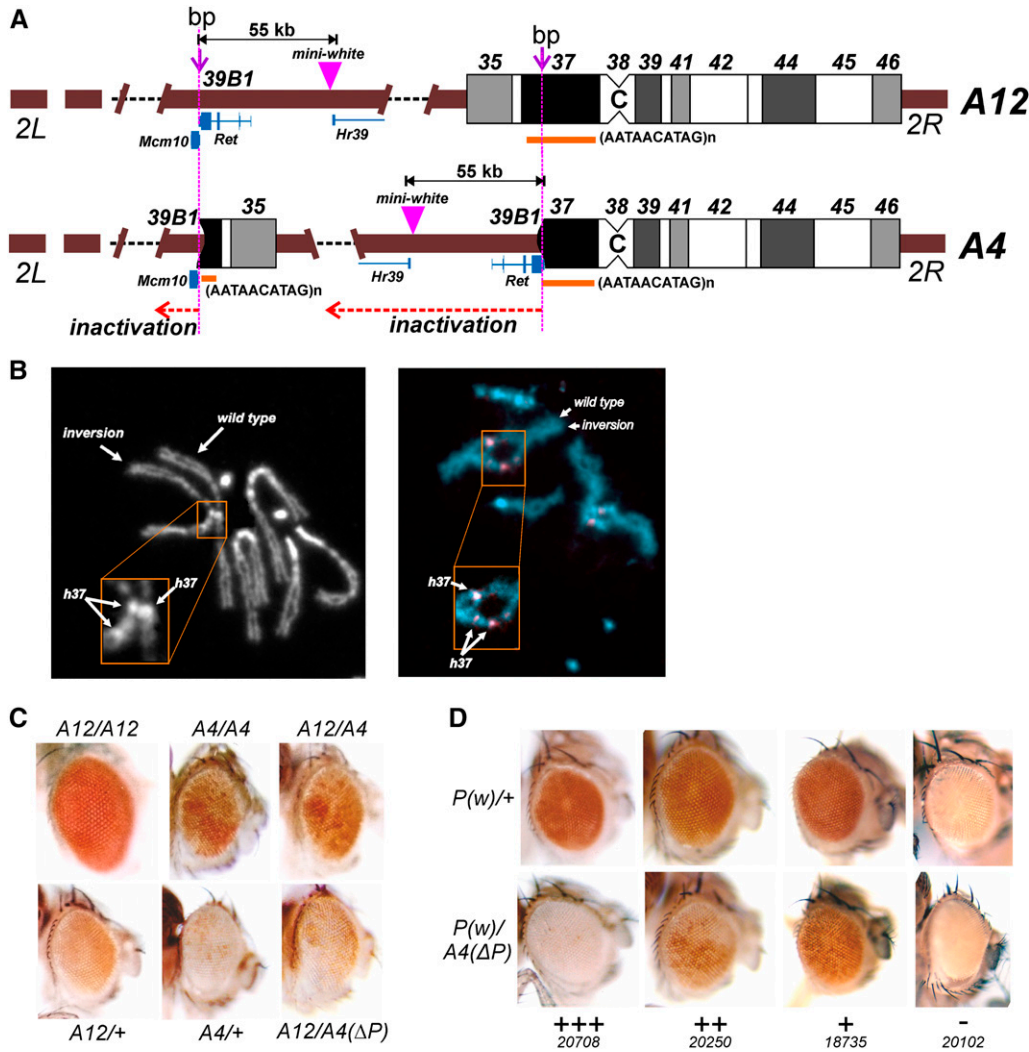


Figure 1 Structure of the A4 rearrangement and the manifestation of *cis*- and *trans*-inactivation of *mini-white* in reporter transgenes. (A) Structure of the A4 chromosome. Breakpoint positions (bp) in euchromatin and heterochromatin are located in the second exon of the *Mcm10* gene and in the *h37* heterochromatin block [according to Dimitri (1991)], respectively. C, centromere. The purple triangle designates the *mini-white*-containing P-element in the *Hr39* gene. Dashed arrows show the spreading of inactivation caused by the main heterochromatic block and the detached small block of heterochromatin. (B) Localization of the heterochromatic breakpoint in A4. (Left) DAPI staining of mitotic chromosomes from A12/A4 larval brains. (Right) *In situ* hybridization using the (AATAACATAG)_n probe (red). The positions of the *h37* block are marked on chromosome 2. (C) Eye color phenotypes resulting from the expression of *mini-white* in the P-element inserted into the *Hr39* gene. The A4 inversion leads to mosaic repression of *mini-white* in A4/+, A4/A4, A12/A4, and A12/A4(ΔP) flies. Dosage effect is seen in A12/A12, A4/A4, and A12/A4 flies. (D) *trans*-inactivation of the *mini-white* reporter (*P(w)*) on normal chromosome 2 in heterozygous *P(w)/A4(ΔP)* flies. The degree of

trans-inactivation is ranked into four categories (+++, ++, +, -) according to the observed degree of *mini-white* repression. The examples of *trans*-inactivation phenotypes of four transgene insertions (20708, 20250, 18735, and 20102) are shown. *P(w)/+* is a *mini-white* reporter over a wild-type chromosome; *P(w)/A4(ΔP)* is the same transgene over an A4(ΔP) chromosome.

AGO2 mutations *AGO2*⁴¹⁴ and *AGO2*^{51B} (chromosome 3) are viable and fertile in homozygous or *trans*-heterozygous states. Flies *P(w)/CyO*; *AGO2*^{*}/TM3, *Sb Ser* and *A4/CyO*; *AGO2*^{*}/TM6U were generated and crossed to get *P(w)/A4*; *AGO2*^{*}/*AGO2*^{*} and *P(w)/A4*; *AGO2*^{*}/TM3, *Sb Ser* (control) males.

To test the *Su(var)2-5* (*HP1a*) effect, the recombinant chromosome *Su(var)2-5*⁰¹, A4 was generated. Males *w^{m4h}/Y*; *Su(var)2-5*⁰¹/SM1, *CyO* were crossed to females *yw/yw*; *A4/SM1*, *CyO*; then the F₁ females *w^{m4h}/yw*; *A4/Su(var)2-5*⁰¹ were crossed to males *yw/Y*; *A4/SM1*, *CyO*. The F₂ recombinant females *yw/yw*; *Su(var)2-5*⁰¹, *A4/SM1*, *CyO* were selected and crossed to males *yw/Y*; *P(w)/SM1*, *CyO*. Eye colors of *yw/Y*; *Su(var)2-5*⁰¹, *A4/P(w)*, and *yw/Y*; *P(w)/Su(var)2-5*⁰¹ males were compared.

RNA-Seq analysis

RNA samples were prepared from 2- to 3-day-old adult or third instar larval females of genotypes A12/A12 and A4/A4

reared at 18°. Homozygous nonfluorescent A4/A4 female larvae were picked from the A4/*CyO-GFP* stock. Samples were prepared according to the standard Illumina protocol [TruSeq RNA Sample Prep Kit after rRNA depletion by RiboZero rRNA Removal Kit (Human/Mouse/Rat), Epicentre] and sequenced on the Illumina HiSeq2000 (Laboratory of Evolutionary Genomics, Moscow State University). The following sequencing parameters were used: two biological replicates of each genotype and stage, single-end reading, read length 50 bp, and number of reads for each sample ~2 × 10⁷.

Raw reads were processed on a local Galaxy instance. The workflow included preprocessing of reads (FASTQ grooming, adapter removal, and quality trimming), transcript assembly, and gene-expression-level quantification by TopHat 0.6 and Cufflinks 0.0.7 using the dm3/R5 *Drosophila* gene set. The Cufflinks output tables with gene-level FPKM values (number of fragments per kilobase of assembled transcript per million fragments mapped to the transcriptome) were processed in

Excel. Genes with zero FPKM or with three times or more FPKM difference between replicates were removed, and the average FPKM values were used for $\log_2(A4/A12)$ calculation.

Next-generation sequencing (NGS) data are available under accession number GSE71842 at the NCBI Gene Expression Omnibus (GEO) website (<http://www.ncbi.nlm.nih.gov/geo>).

Messenger RNA (mRNA) quantification

mRNA abundances for the genes near the A4 breakpoints were evaluated by real-time quantitative polymerase chain reaction (RT-qPCR). RNA was extracted from 2- to 3-day-old adult females or third instar female larvae A12/A12 and A4/A4 reared at 18° using the RNeasy Mini Kit (Qiagen). RNA was reverse transcribed with random hexamer primers. Evaluation of the normalized relative quantities ($\Delta\Delta C_q$) of transcripts was performed by real-time PCR using gene-specific primers and a DT-96 amplifier (DNA-Technology LLC). mRNA quantities in the samples were normalized to that of the housekeeping *RpL32* gene transcript. \log_2 -transformed ratios of A4 to A12 transcript amounts were calculated from the three biological replicates. Average values and SDs are presented in the figures and in Table S3. The oligonucleotides used are listed in Table S2.

Chromatin immunoprecipitation (ChIP)

ChIP was performed as described previously (Klenov *et al.* 2007). Chromatin was extracted from third instar larvae and precipitated with antibodies against HP1a (Covance catalog #14923202) and H3K4me2 (Millipore #07-030). Two independent biological replicates were made. The enrichments were analyzed by RT-qPCR using a reference region 60D (chr2R:20322299–20322469) for sample quantity normalization. Primers used in ChIP measurements are listed in Table S2.

In situ hybridization and immunostaining

Mitotic chromosomes were prepared from A4/A12 and A12/A12 larval brains fixed according to Gatti *et al.* (1994) and mounted with a DAPI-containing medium (VECTASHIELD). Biotinylated oligonucleotides Biot-(AACAC)₁₀, Biot-(GAGAA)₁₀, and Biot-(AATAACATAG)₅ were used for *in situ* hybridization to reveal satellite DNA blocks on mitotic spreads. Mitotic chromosomes were stained with DAPI, and biotin signals were detected by Streptavidin, Alexa Fluor 546 (Life Technologies) under a fluorescent microscope.

Combined fluorescent immunostaining of proteins and DNA *in situ* hybridizations were performed according to a published protocol (Shpiz *et al.* 2014). Imaginal disks and salivary glands were isolated from the third instar larvae and hybridized to a biotinylated oligonucleotide probe for the AACAC satellite (chromosome 2 pericentromeric heterochromatin), a DIG-labeled probe for the 25-kb 39AB region (chr2L:21150645–21182675), and a Cy5-labeled probe for the histone gene cluster. The DIG-labeled probe for the

39AB region was generated by random priming of long-range PCR-amplified fragments from this region using DIG DNA Labeling Mix (Roche). The probe for the histone gene cluster was prepared by random priming of the PCR-amplified histone gene cluster unit (*His1* to *His3*) using a Cy5-labeled nucleotide. *In situ* hybridization was combined with polyclonal rabbit anti-HP1a staining (PRB-291C, Covance). Results of hybridization and immunostaining were visualized by Streptavidin, Alexa Fluor 546 (Life Technologies) for AACAC, anti-DIG-FITC AB (Roche) + anti-FITC Alexa 488 (Life Technologies) for the 39AB probe, and anti-rabbit–Alexa 514 conjugate (Life Technologies) for HP1a. The histone gene probe signal was detected by Cy5 fluorescence. Samples also were stained with DAPI to visualize nuclei. Oligonucleotides used for probe synthesis are listed in Table S2.

Samples were mounted in Slow Fade Medium (Invitrogen) for imaging in a Carl Zeiss LSM510 Meta Confocal Microscope equipped with a spectra analyzer and lasers of 405 (DAPI), 488 (FITC), 514, 546, and 633 nm. Three-dimensional (3D) images of stained nuclei were quantified in Imaris 7 software (Bitplane). The spots objects were generated in AACAC (histone gene cluster) 39AB probe *in situ* signal channels, and the mean intensity in the HP1a channel was calculated for each spot. The total number of treated nuclei was 100 for each genotype, and the average values and SDs for each *in situ* probe were calculated.

Software tools

We used local mirrors of the UCSC Genome Browser (<https://genome.ucsc.edu>) and Galaxy (<https://usegalaxy.org>) for data treatment and visualization. Custom tracks of the A4 breakpoint position, positions of checked transgenes with color information representing sensitivity to *trans*-inactivation, and positions of probes for qPCR and *in situ* hybridization were created in BED (.bed) format, uploaded to the UCSC Genome Browser, and used for creation of the figures. Confocal image processing and calculations were done in Imaris 7.

Data availability

Created fly stocks are available upon request. Table S1 contains the list of fly lines bearing insertions used in the study. Stocks IDs are supplied. Table S2 contains the sequences of used primers. Table S3 contains treated NGS and qPCR data, Table S4 lists the alleles used in the study. Gene expression data are available at GEO with the accession number: GSE71842.

Results

Structure of A4 rearrangement

Inversion A4 was produced by X-ray irradiation of the A12 chromosome carrying a *mini-white*-containing *P*-element insertion. Irradiation caused two breakpoints, one in the 39B1 euchromatic section and the other in the pericentromeric

heterochromatin of chromosome 2. The euchromatic breakpoint was localized to a 105-bp region (chr2L:21182214–21182318) of the second exon of the *Mcm10* gene using conventional genomic Southern blotting and PCR analysis (data not shown). The position of the heterochromatin breakpoint was revealed using differential staining of mitotic chromosomes from *A12/A4* individuals. The heterochromatic *h37* DAPI-bright region (Dimitri 1991) is split in *A4* into two parts, the larger part remaining at the centromere and the smaller part relocated to euchromatin (Figure 1, A and B). *In situ* fluorescence hybridization with several labeled satellite probes confirmed the cytologic localization of the heterochromatic breakpoint within the *h37* region containing the (AATAACATAG)_n dodecasatellite (Lohe *et al.* 1993). Approximately one-third of the *h37* block is relocated to euchromatin.

A4 inversion results in two new euchromatin-heterochromatin borders—the border between euchromatin and a small, separated heterochromatin block (*h35–h37*) and the border between euchromatin and the main block of pericentromeric heterochromatin of chromosome 2. Euchromatin sections 39B2–40F are inverted relative to normal chromosome orientation and placed between two heterochromatin blocks (Figure 1A).

Evaluation of cis-effects of heterochromatin in *A4*

The *A12* chromosome, the progenitor of the *A4* inversion, carries the *mini-white*-containing *P*-element in the 5' UTR of the *Hr39* gene. Flies of genotype *A12/A12* have 10 times more eye pigment (quantitative data not shown) compared to *A12/+* flies, while the gene dosage increases just twice (Figure 1C). In the *A4* chromosome, the *mini-white* transgene is located 55 kb from the new euchromatin-heterochromatin border and demonstrates a strong variegated expression in both *A4/+* and *A4/A4* flies (Figure 1C). The eye color in *A4/A4* flies is significantly more intense than in *A4/+* flies, similar to the eye color difference between *A12/A12* and *A12/+* flies. The observed dosage effect of the expression of *mini-white* is specific to transgenes inserted at the beginning of the *Hr39* gene and is beyond the scope in this paper.

Variegated expression of the *mini-white* reporter in *A4/+* and *A4/A4* flies points to PEV caused by rearrangement. The effects of heterochromatin on neighboring euchromatic genes and the distance of inactivation spreading were evaluated using RNA-Seq analysis of the gene expression in *A4/A4* and *A12/A12* (control) larvae and adult females. qPCR verification of RNA-Seq data is presented for a set of genes scattered over a 500-kb region near the pericentromeric heterochromatin (39AE region) and a 50-kb region adjacent to the detached heterochromatic block (Figure 2 and Table S3). These regions in the normal chromosome demonstrate *trans*-inactivation of *mini-white* reporters when heterozygous with *A4* (see later). Thirty-four genes in the selected region have expression levels high enough for reliable quantification. The log₂-transformed *A4/A4*-to-*A12/A12* ratio values for these genes are presented in Figure 2B.

In the region adjacent to the main (centromeric) heterochromatin, we found the only three genes showing a significant decrease (greater than twofold according to both RNA-Seq and qPCR) in mRNA abundance in *A4/A4* larvae compared to *A12/A12* larvae. These genes are located 35 kb (*CG8678* and *CG8679*) and 63 kb (*Hr39*) from the heterochromatin. In *A4/A4* adults, no decrease in *CG8679* and *Hr39* expression was observed, and a slightly increased expression of *CG8678* was detected. Surprisingly, the *CG8665* gene (189 kb from heterochromatin) demonstrated a strong fourfold activation at the larval stage in *A4/A4* larvae. In the region adjacent to the small, detached block of heterochromatin, we found a twofold increase in *Acon* gene expression in *A4/A4* larvae (13.5 kb from the breakpoint). No significant changes in gene expression in *A4/A4* compared to *A12/A12* flies were found at the adult stage.

Thus, analysis of gene expression at the euchromatin-heterochromatin border in *A4/A4* flies allows us to conclude that only a few genes respond to heterochromatin proximity, and their susceptibility to the effects of heterochromatin can vary at different developmental stages (*e.g.*, for the *CG8678* gene at the larval and adult stages) (Figure 2B). Some genes even demonstrate an increased expression, while the majority of euchromatic genes near the heterochromatin remain unaltered or demonstrate very small changes in expression.

We checked the chromatin state of the genes affected by PEV (*Acon*, *CG8678*, *CG8679*, *Hr39*, and *crc* as a negative control) by ChIP with anti-HP1a and anti-H3K4me2 antibodies. HP1a is a marker of heterochromatin, while the H3K4me2 histone modification associates with active transcription. Chromatin samples were prepared from *A12/A12* and *A4/A4* larvae, and the log₂-transformed ratios of *A4/A4* to *A12/A12* enrichments in HP1a and H3K4me2 were calculated. Significant enrichments in HP1a (greater than twofold) were detected at the repressed *CG8679* and *Hr39* genes, while no changes occurred at the activated *Acon* or *crc* gene with an unchanged level of expression. A weak enrichment (1.5-fold) in HP1a was detected for the repressed *CG8678* gene. Changes in H3K4me2 were insignificant in all cases (Figure 2C). Thus, the increase in HP1a abundance underlies heterochromatin-caused *cis*-repression in tested genes.

Trans-Inactivation of *mini-white* reporters caused by *A4* rearrangement

We noticed that *A12/A4* flies demonstrate variegated eye color (Figure 1C), while *A12/A12* or *A12/+* flies have uniformly colored eyes. The same variegated phenotype is observed in *A12/A4(ΔP)* flies carrying the inversion lacking the *mini-white* transgene (Figure 1C). This observation points to the ability of the *A4* inversion to inactivate genes on the homologous normal chromosome (*trans*-inactivation). To evaluate the area of *trans*-inactivation, we checked 69 *mini-white*-containing transgenes (see *Materials and Methods* and Table S1) scattered throughout the 38D–40F region for their susceptibility to *trans*-inactivation by the *A4* rearrangement.

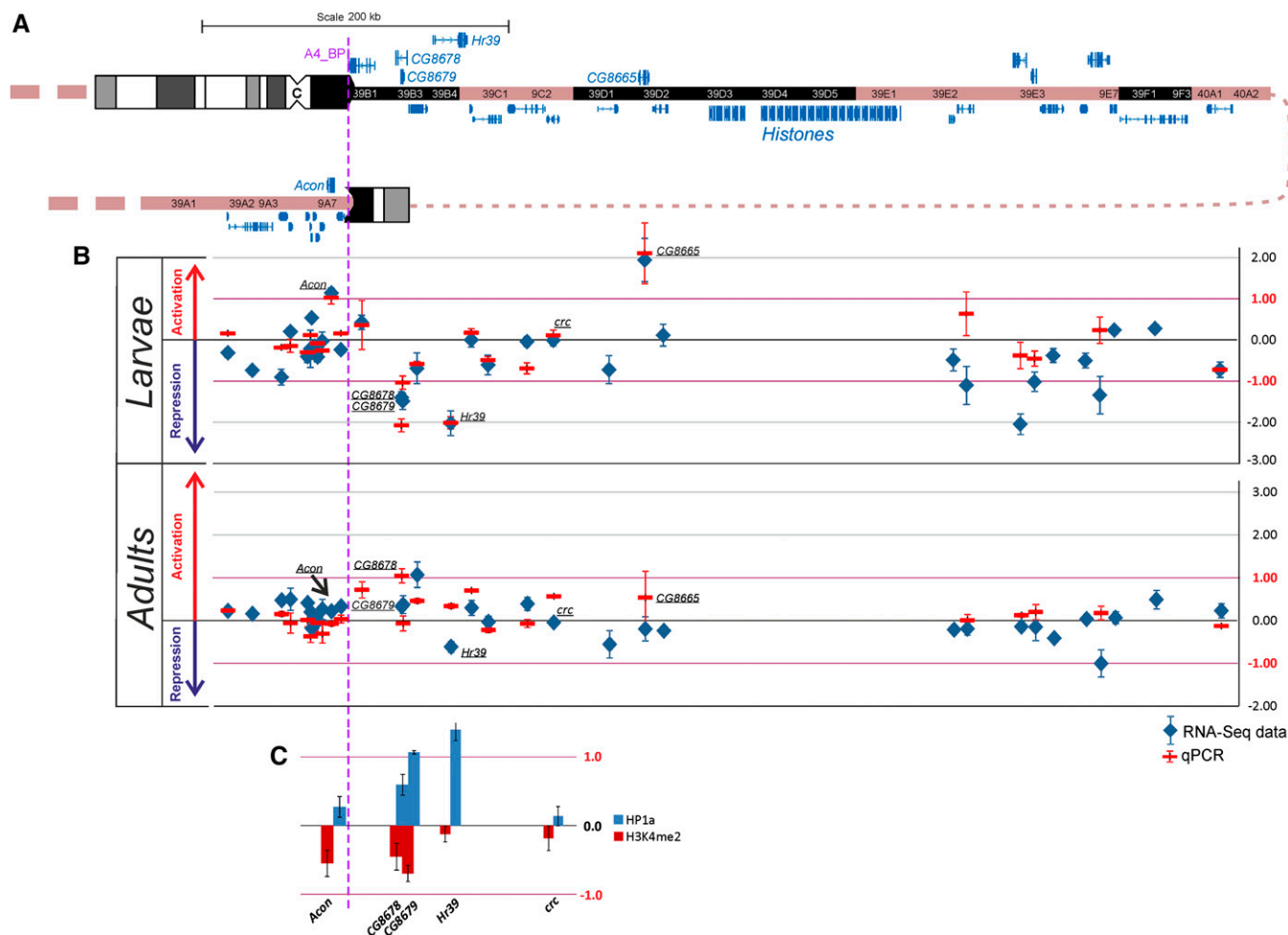


Figure 2 *cis*-Effects of heterochromatin in the A4 inversion in larvae and adults. (A) Structure of the A4 inversion. C, centromere. Black, gray, and white blocks represent the organization of heterochromatin of chromosome 2 (Dimitri 1991). Exon-intron maps of the genes in the region are presented, and the genes with confirmed greater than twofold expression changes in either larvae or adults have captions. Euchromatic position of the A4 breakpoint is shown by the vertical dotted line. (B) Chromosome distributions of \log_2 -transformed ratios (A4/A4 to A12/A12) of normalized gene expression levels based on RNA-Seq (blue diamonds) and qPCR (horizontal red strips) data. *cis*-Repression corresponds to negative values. These data show that euchromatic genes respond to heterochromatin-induced *cis*-effects individually and differently in larvae and adults. (C) Changes in HP1a and H3K4me2 abundance (\log_2 -transformed A4/A4-to-A12/A12 ratio) for the genes *Acon*, *CG8678*, *CG8679*, *Hr39*, and *crc* at the larval stage. The positions of the bars correspond to the positions of genes on the chromosome. Genes *Acon*, *CG8678*, *CG8679*, *Hr39*, but not *crc* change their expression near the heterochromatin (B). Significant changes (greater than twofold) in HP1a are detected for the *Hr39* and *CG8678* genes, and no significant difference is observed for H3K4me2 enrichments.

These transgenes are located in the 1.5-Mb region (38D–40F) around the position corresponding to the euchromatic breakpoint in A4.

A4 induces *trans*-inactivation of the *mini-white* reporters, and the *trans*-inactivation exhibits uneven distribution over a wide area starting from the position of the euchromatic breakpoint in A4. Two distinct areas of *trans*-inactivation were detected; the first, smaller one is homologous to the euchromatic region adjacent to the separated small heterochromatin block in A4 (Figure 3, region A), and the second, much more extended one corresponds to the euchromatic part of chromosome 2L transposed to pericentromeric heterochromatin in A4 (Figure 3, regions B, C, and E). *trans*-Inactivation in region A spreads over a distance of approximately 40 kb, while the second area encompasses 476 kb

because inactivation of the 19883 transgene located in the 39E3 region is detectable (Figure 3, region E, bold). An irregular pattern of *mini-white trans*-inactivation was found in the second area. Continuous repression is observed in the 40-kb region adjacent to the centromeric heterochromatin (region B), which is followed by the 80-kb region of interspersed inactivation (region C), where some transgenes are turned off and others are active. No *trans*-inactivation was detected near the histone gene cluster (region D), but we found an ~45-kb “island” of *trans*-inactivation after the histone gene cluster (region E).

A4 inversion induces repression of *mini-white* reporters on the homologous normal chromosome. In the region near the euchromatin-heterochromatin border (~40 kb in size), transgenes of any tested type in any position could be

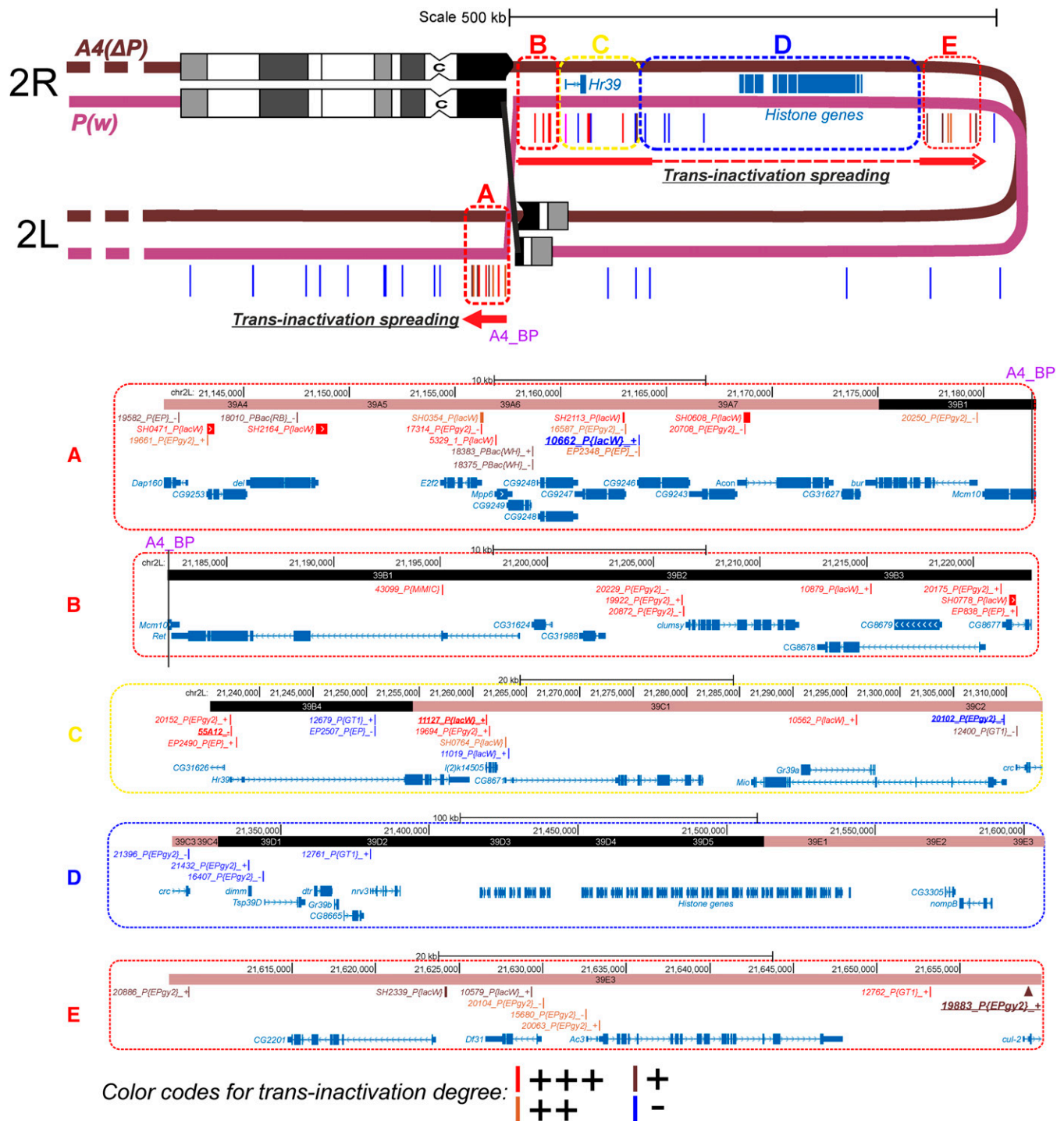


Figure 3 Detailed map of *mini-white* reporter *trans*-inactivation in $A4(\Delta P)/P(w)$ flies. (Top) Schematic representation of paired $A4(\Delta P)$ and transgene-bearing $P(w)$ chromosomes forming an inversion loop. The $A4(\Delta P)$ chromosome contains pericentromeric and detached smaller heterochromatin blocks that cause propagations of *trans*-inactivation (shown by thick red arrows). Colored vertical strokes represent the positions and degree of transgene repression: red, strong inactivation; orange, moderate inactivation; brown, weak inactivation; and blue, no inactivation. The whole area of *trans*-inactivation spreading is subdivided into regions of total repression (A and B with the single exception of 10662), moderate/interpersed repression (C and E), and no repression (D) of inserted transgenes. Dashed colored lines outline the approximate borders of these regions. (Bottom) Close-up views of regions A, B, C, D, and E showing the positions of endogenous genes and transgene insertions. Transgene names are constructed as “stock number_transgene type_insertion orientation”; the colors of transgenes correspond to the degree of repression, as in the top panel. Regions A and B, ~40 kb each, are immediately adjacent to heterochromatin in the $A4$ chromosome. Region C is the region of interspersed inactivation (~80 kb). Region D includes the histone gene cluster; no *trans*-inactivation is observed here. Region E is the “island” of *trans*-inactivation after the histone gene cluster. The furthestmost transgene still repressed is 19883 (region E, 475 kb from the breakpoint position).

trans-inactivated, in contrast to *cis*-repression of euchromatic genes near the A4 breakpoint.

HP1a occupancies at the *trans*-inactivated transgene are independent of chromatin state at homologous sites on the A4 chromosome

A comparison of *cis*-effects of heterochromatin on a given gene in A4 and *trans*-inactivation of the transgene inserted into this gene on the homologous chromosome reveals no correlation between the two effects. For instance, the *Acon* gene demonstrates *cis*-activation in A4/A4 larvae, while the 20708 insertion in its 5' UTR is strongly *trans*-inactivated (Figure 2 and Figure 3). We suggest that the formation of repressive chromatin in the transgene occurs independently of the chromatin state of the homologous region on A4. To check this assumption directly, we compared HP1a enrichments inside the transgenes and at the sites of transgene insertion on the A4(Δ P) chromosome by ChIP.

We checked the chromatin state of the two transgenes, *trans*-inactivated 11127 (*P*[*lacW*] in *l(2)k14505*) and non-inactivated 20102 (*P*[*EPgy2*] in *Mio*). Samples were prepared from the *w*^{*}; 11127/A4(Δ P), *w*^{*}; 20102/A4(Δ P), and *w*^{*}; 11127/+ , *w*^{*}; 20102/+ (control) third instar larvae because *mini-white* expression starts at this developmental stage, and the most prominent effects of heterochromatin on gene expression were observed in the larvae based on RNA-Seq data.

Figure 4 presents the design of the experiment, including the positions of the primers used. Primers to *mini-white* and *LacZ* genes were applied for HP1a and H3K4me2 enrichment measurements in insertion 11127. There is no *LacZ* in insertion 20102; just primers to *mini-white* were used in this case. To measure the occupancies of HP1a and H3K4me2 at the sites on the A4(Δ P) chromosome corresponding to the place of 11127 transgene insertion, we used a primer pair designated as 11127. The PCR product from this primer pair overlaps the place of insertion of the respective transgene (Figure 4).

We found more than a twofold enrichment in HP1a at the *mini-white* and *LacZ* genes in *trans*-inactivated transgene 11127 (in 11127/A4(Δ P) relative to the 11127/+ control). The changes in the H3K4me2 modification level were insignificant, with a tendency to drop at *LacZ* (Figure 4B, lower histogram). No significant enrichments of HP1a or H3K4me2 were detected at the *mini-white* gene of noninactivated transgene 20102 (in 20102/A4(Δ P) relative to the 20102/+ control) (Figure 4C, lower histogram).

The site opposite the 11127 transgene on the A4(Δ P) chromosome showed no significant enrichments in HP1a in the absence of this transgene (in 20102/A4(Δ P) relative to the 20102/+ control) (Figure 4C, top histogram). However, in the presence of the transgene (in 11127/A4(Δ P) larvae), HP1a enrichment was detected on the A4(Δ P) chromosome in the place of the 11127 transgene insertion (Figure 4B, top histogram). Since the HP1a accumulates at the 11127 in 11127/A4(Δ P) (as mentioned earlier), we suggest that the

heterochromatinization of the transgene occurs *de novo* and is not caused by HP1a spreading from neighboring regions. The heterochromatinization of the *trans*-inactivated transgene probably induces the accumulation of HP1a on the opposite site on the homologous chromosome. Results of ChIP experiments demonstrate that the *trans*-inactivated transgene binds HP1a and that autonomous heterochromatinization of the transgene could induce the accumulation of HP1a on the opposite chromosome.

Trans-Inactivation and the nuclear position of the histone cluster

The small, detached heterochromatin block in the A4 chromosome tends to conjugate with the pericentromeric heterochromatin in A4/A4 flies and is able to drag regions of somatically paired normal chromosome (in A4/+ flies) into the heterochromatic nuclear compartment (Abramov *et al.* 2011; Lavrov *et al.* 2013; unpublished data). Inversion A4 produces a peculiar pattern of *mini-white* transgene *trans*-inactivation along the chromosome: repression occurs on both sides of the histone gene cluster, while several transgenes (21396, 21432, 16407, and 12761) (Figure 3, region D) located close to the cluster show no *mini-white* repression. To check the correlation of this effect with a specific nuclear compartmentalization of the histone gene cluster, we performed combined *in situ* hybridization and HP1a immunostaining of nuclei from A12/A12 and A12/A4 larval imaginal disks. The heterochromatic compartment was detected by HP1a staining, and the intranuclear positions of chromosome regions were visualized using DNA probes for the 39AB region (35-kb fragment immediately adjacent to the euchromatic breakpoint), the histone gene cluster, and the AACAC satellite as a marker of pericentromeric heterochromatin of chromosome 2. One hundred interphase nuclei of both genotypes were analyzed using a confocal microscope.

The number of signals for each hybridization probe per nuclei and the position of each probe relative to an HP1a-stained subvolume of nuclei volume were estimated. Single spots for the 39AB region and the histone gene cluster were revealed in 92% of A4/A12 nuclei and 94% of A12/A12 nuclei. These data indicate the essentially complete pairing of homologs both in the case of normal chromosomes (A12/A12) and in *trans*-heterozygous combinations of normal and rearranged chromosomes (A4/A12).

We found that the histone gene cluster localizes in both A4/A12 and A12/A12 nuclei at the border of the highly enriched HP1a area (97% of nuclei). The 39AB fragment, representing the *trans*-inactivated area, locates in the euchromatin in A12/A12 nuclei, while in A12/A4 nuclei it is detectable inside the HP1a-stained compartment (Figure 5). To confirm this observation, measurements of the mean intensities of HP1a staining at the positions of *in situ* hybridization signals of the AACAC satellite, the histone gene cluster, and the 39AB region were performed (described in *Materials and Methods*). The measurements show that the concentration of

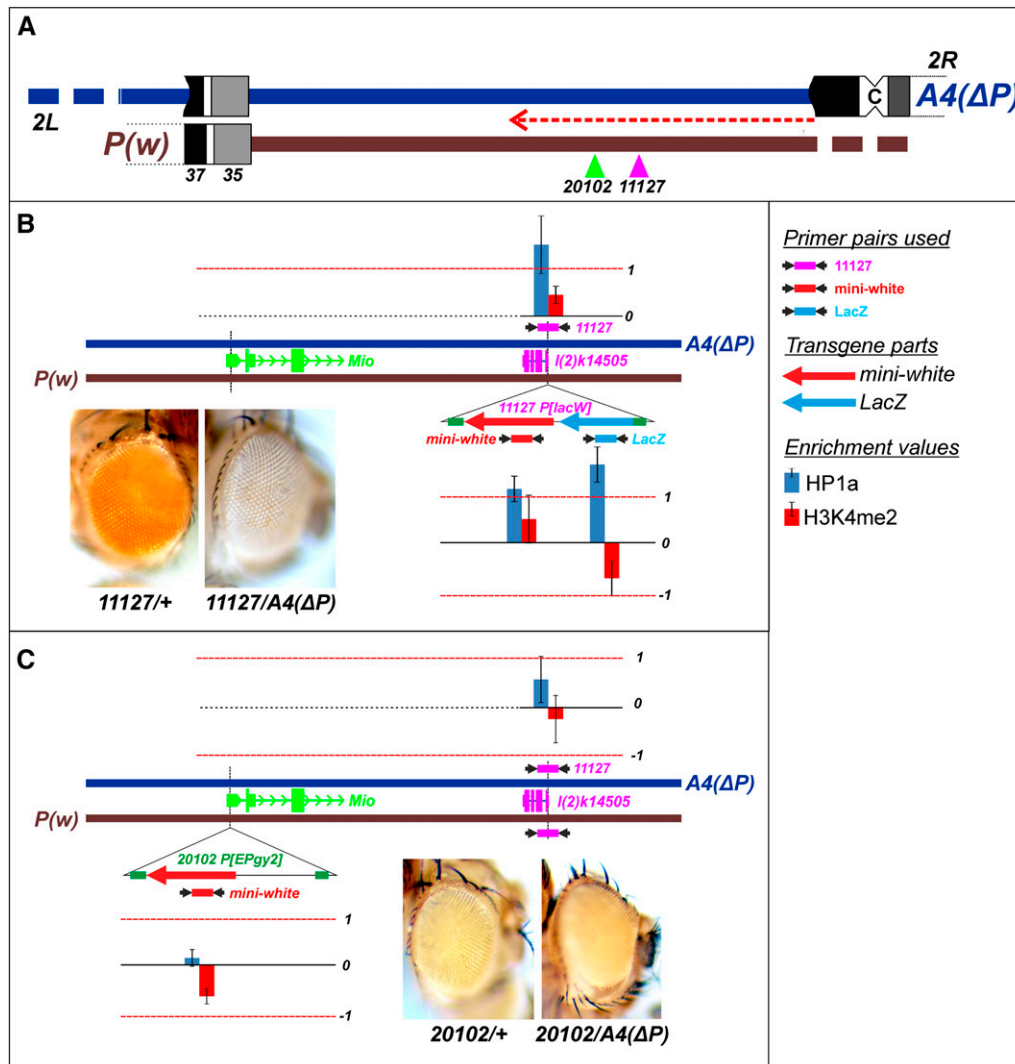


Figure 4 HP1a accumulates at the *trans*-inactivated transgene and on A4 at the site homologous to insertion of the *trans*-inactivated reporter. Primer pairs used for ChIP analysis of the transgenes (*mini-white*, *LacZ*) and the site on the A4(ΔP) chromosome corresponding to transgene insertion 11127 are marked by different colors. The histogram bars in B and C presents the log₂-transformed ratios of HP1a (blue) or H3K4me2 (red) abundance in *P(w)/A4(ΔP)* individuals to *P(w)/+* individuals; the bar positions correspond to the locations of the regions analyzed. The *trans*-inactivation phenotypes are shown for 11127 and 20102. (A) Fragments of A4(ΔP) inversion and normal *P(w)* chromosome carrying reporter transgenes. The direction of *trans*-inactivation spreading along the nonrearranged chromosome is indicated by the red dotted arrow. The positions of the 11127 (*trans*-inactivated) and 20102 (noninactivated) transgenes are indicated by pink and green triangles, respectively. (B) *trans*-inactivated insertion 11127 in 11127/A4(ΔP) larvae. The scheme shows the arrangement of the 11127 and A4(ΔP) chromosomes, positions of insertion and primers, and the simplified structure of the *P[lacW]* transgene inserted (below the chromosome). The positions of histogram bars showing the HP1a and H3K4me2 enrichment levels correspond to the positions of primers. HP1a accumulates at the constituents of *trans*-inactivated transgene 11127 (histogram below the transgene image) and in the site of this transgene insertion on the opposite A4(ΔP) chromosome (primers 11127). (C) Noninactivated insertion 20102 in 20102/A4(ΔP) larvae (for designations, see B). No accumulation of HP1a in the *mini-white* of transgene 20102 was observed. There was also no accumulation of HP1a in the site of transgene 11127 insertion in the absence of the proper transgene. A significant enrichment in HP1a was observed in *trans*-inactivated but not in noninactivated transgenes. The comparison of chromatin state on A4(ΔP) when heterozygous with the *trans*-inactivated transgene reveals an HP1a enrichment.

ment levels correspond to the positions of primers. HP1a accumulates at the constituents of *trans*-inactivated transgene 11127 (histogram below the transgene image) and in the site of this transgene insertion on the opposite A4(ΔP) chromosome (primers 11127). (C) Noninactivated insertion 20102 in 20102/A4(ΔP) larvae (for designations, see B). No accumulation of HP1a in the *mini-white* of transgene 20102 was observed. There was also no accumulation of HP1a in the site of transgene 11127 insertion in the absence of the proper transgene. A significant enrichment in HP1a was observed in *trans*-inactivated but not in noninactivated transgenes. The comparison of chromatin state on A4(ΔP) when heterozygous with the *trans*-inactivated transgene reveals an HP1a enrichment.

HP1a at the position of 39AB is higher in A4/A12 nuclei than in A12/A12 nuclei and that the concentration of HP1a in the position of the histone gene cluster remains approximately the same in A4/A12 and A12/A12 nuclei but is lower than at the position of the AACAC satellite (Figure 5C).

The 39AB probe, which corresponds to region A of continuous *trans*-inactivation (Figure 3), produces a single hybridization spot in most A4/A12 nuclei. Region A is normally (in A12/A12 nuclei) located in euchromatin and is dragged into the HP1a-rich compartment in A4/A12 nuclei. The probe for the histone gene cluster corresponds to region D, where no *trans*-inactivation is observed (Figure 3). Despite the conjugation of A4 with A12, the histone gene cluster tends to be excluded from the heterochromatic compartment to the border of the HP1a-enriched area. We assume that the histone gene

cluster stays out of the heterochromatic compartment, thus suppressing *trans*-inactivation in its vicinity.

Genetic modifiers of *trans*-inactivation

We tested several well-known modifiers of PEV for their ability to affect *trans*-inactivation (see *Materials and Methods* and Table S4). The eye phenotypes in Figure 6 are presented for transgene 11127, located in region D with interspersed *trans*-inactivation (Figure 3).

Most traditional PEV modifier mutations tested (*i.e.*, *Su(var)2-5*, *Su(var)3-1*, *Su(var)3-6*, and *Su(var)3-7*) suppress *trans*-inactivation of transgenes and *cis*-inactivation of the reporter *mini-white* inserted in the *Hr39* gene in A4 (Table S4). The exception is the mutations in the *Su(var)3-9* gene, which have no effect on *trans*- or *cis*-inactivation of *mini-white* in the A4

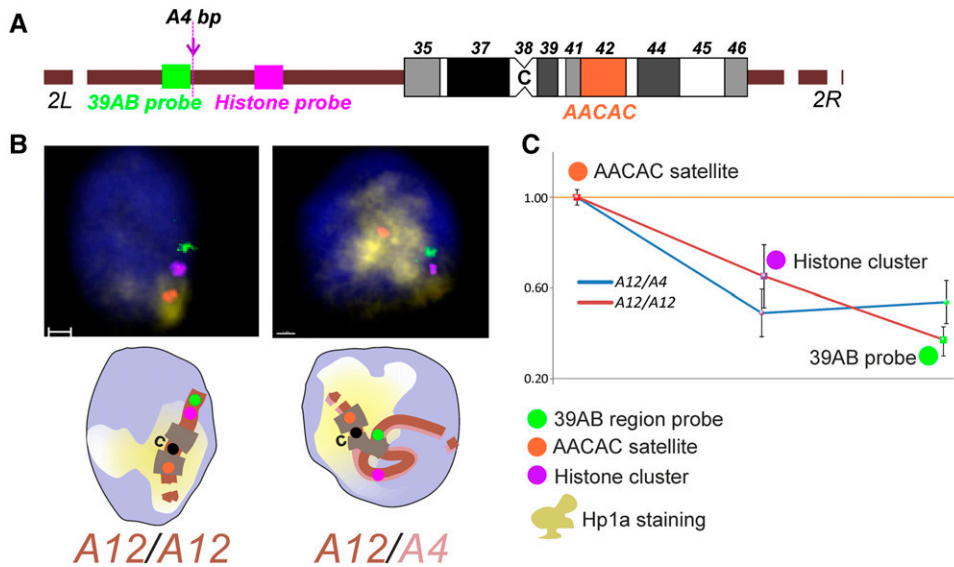


Figure 5 The 39AB region located in A12/A12 nuclei in euchromatin is moved to the heterochromatic compartment in A12/A4, while the histone gene cluster maintains its position at the euchromatin-heterochromatic border. (A) The positions of the *in situ* probes for 39AB (green), histone gene cluster (pink), and AACAC satellite (red) are shown on a schematic chromosome 2 map. The arrow points to the position of the A4 breakpoint. (B) Examples of confocal nuclei cross section and the schematic view (below) of paired homologous chromosomes of typical A12/A12 and A12/A4 nuclei after *in situ* staining. C, centromere. Colored dots on the scheme represent the positions of the *in situ* hybridization probes; their colors correspond to those of the FISH signals on the confocal images and on the chromosome scheme at the top. The yellow

cloud is HP1a staining of the heterochromatin compartment. (C) Mean HP1a staining intensities calculated at the positions of *in situ* signals of the histone gene cluster and the 39AB region and normalized to the mean intensity of HP1a staining at the position of the AACAC satellite signal.

chromosome. The *Su(var)3-9* gene encodes histone methyltransferase, one of the key components of the heterochromatin-spreading mechanism (Schotta *et al.* 2002). However, mutation in the *eggless* gene encoding another histone methyltransferase, SETDB1, strongly suppresses *trans*-inactivation of transgenes as well as *cis*-inactivation of *mini-white* in A4 (not shown).

We detected opposite effects on *trans*-inactivation of two proteins known to be involved in chromatin state maintenance. *trans*-Inactivation but not *cis*-inactivation of *mini-white* in A4 is strongly suppressed by the *e(y)3^{u1}* mutation affecting the supporter of activation of yellow protein [SAYP, a coactivator/subunit of the Brahma remodeling complex (Chalkley *et al.* 2008) and an essential component for heterochromatin establishment on chromosome 4 (Shidlovskii *et al.* 2005)]. We also found that the AGO2 protein acts as a potent suppressor of *trans*-inactivation. This protein was earlier described as a component of the insulator complex (Moshkovich *et al.* 2011), and loss of its function disturbed transcription in *Drosophila* (Cernilogar *et al.* 2011). Homozygous (*P(w)/A4; AGO2⁴¹⁴/AGO2⁴¹⁴*) or *trans*-heterozygous (*P(w)/A4; AGO2⁴¹⁴/AGO2^{51B}*) males have white eyes, contrary to their heterozygous siblings, with colored eyes (Figure 6). *AGO2* mutations also exert a smaller but discernible enhancer effect on *cis*-inactivation in A4.

Mutations in genes *UAP56* (a component of mRNA nuclear transport), *zeste* (which affects transvection), and *piwi* (a component of the PIWI-interacting RNA silencing pathway) have no effect on *trans*-inactivation (not shown), although they have been reported as PEV or chromosomal interaction modifiers (Hazelrigg and Petersen 1992; Eberl *et al.* 1997; Pal-Bhadra *et al.* 2004).

Discussion

In this paper, we describe the genetic system inversion A4 in chromosome 2, which provides an opportunity to explore

simultaneously the *cis*- and *trans*-effects of a euchromatin-heterochromatic rearrangement. This inversion was originated by irradiation-induced breakpoints in euchromatin and in the block of dodecasatellite in pericentromeric heterochromatin of the normal progenitor A12 chromosome carrying the *mini-white* reporter. A4 causes a variegated phenotype of the *mini-white* reporter located 55 kb from the border with the main centromeric heterochromatin block. A4 also causes *trans*-inactivation of the *mini-white*-containing transgenes located on the nonrearranged chromosome in regions homologous to those adjacent to heterochromatin in A4 (Figure 1 and Figure 3).

To check the degree of propagation of heterochromatin *cis*-acting effects, we measured the expression levels of genes in A4/A4 and A12/A12 adult and third instar female flies (Figure 2 and Table S3). To our knowledge, this is the first PEV study using RNA-Seq profiling. We found that most euchromatic genes in their natural environment (contrary to reporter transgenes) are resistant to the influence of heterochromatin in the A4 inversion. A significant decrease in mRNA level was shown only for 3 genes (*G8678*, *CG8679*, and *Hr39*) of 34 analyzed genes in A4 larvae, and no significant changes in expression were detected in adults. Our observation that the expression of most heterochromatin-relocated genes is unaltered is similar to the results of an earlier study of *white-mottled* inversions (Vogel *et al.* 2009). These authors demonstrated a notable decrease in the expression of only the *white* gene of 20 tested genes relocated to heterochromatin. The authors suggested that the *white* gene has an unusual intrinsic affinity for heterochromatin, which may render this gene more susceptible to silencing by heterochromatin than most other genes.

Obviously, the *white* gene is not the unique target of PEV. There are a number of examples of PEV of different genes in classical genetics studies (Spofford 1976). In the case of A4

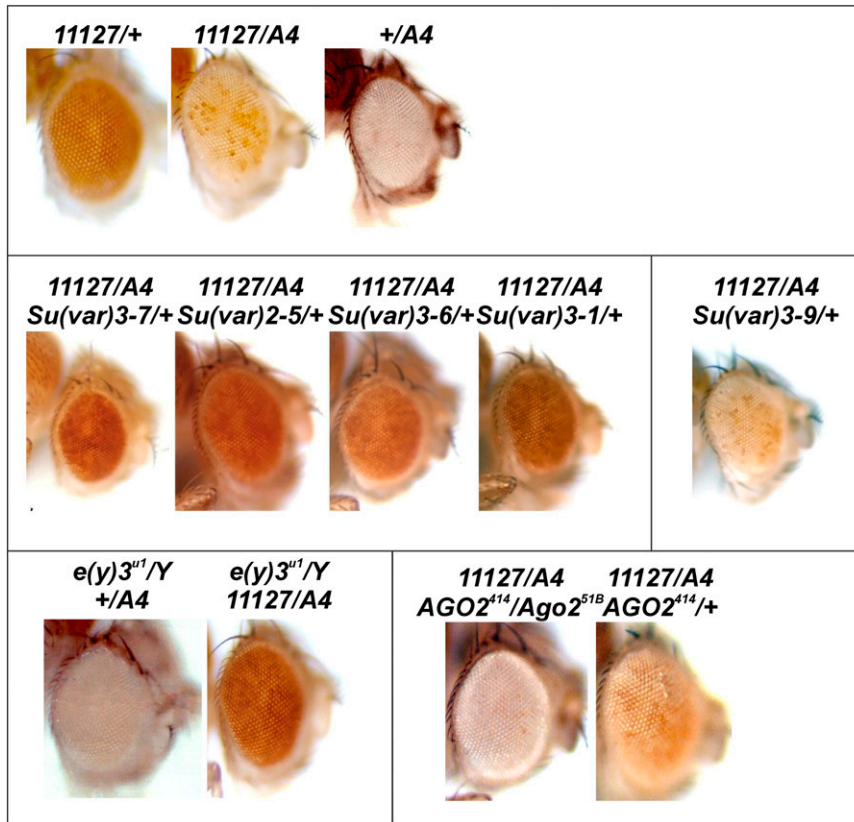


Figure 6 Effect of PEV modifiers and the *e(y)3* transcriptional coactivator on *trans*-inactivation. *trans*-Inactivated transgene 11127 is the insertion of *P[lacW]* at a distance of 80 kb from the border between euchromatin and the pericentromeric block of heterochromatin in *A4*. *Su(var)2-5*, *Su(var)3-7*, *Su(var)3-6*, and *Su(var)3-1* suppress *trans*-inactivation of *mini-white* in 11127/*A4* flies. *Su(var)3-9* does not suppress *trans*-inactivation, while *e(y)3^{u1}* suppresses *trans*- but not *cis*-inactivation. *AGO2* mutations (*AGO2⁴¹⁴*/*AGO2^{51B}* and *AGO2⁴¹⁴*/*AGO2⁴¹⁴* have the same effect) enhance *trans*-inactivation but to a much lesser degree *cis*-inactivation of *mini-white* in *A4*.

rearrangement, three different genes are repressed in heterochromatin proximity. The features making a gene amenable to heterochromatin repression are not known at present, but one possibility could be ruled out in our study. There is no visible correlation between the transcription level of the gene and the degree of repression under the influence of heterochromatin. This follows from a comparison of expression levels of genes in the RNA-Seq data (Table S5).

Surprisingly, we showed not only repression but also activation of two genes located near the heterochromatin in the region visibly heterochromatinized in the *A4* polytene chromosomes (data not shown). Expression of the *Acon* gene (evaluated by both RT-qPCR and RNA-Seq) increased two-fold and expression of the *CG8665* gene increased fourfold in *A4/A4* larvae compared to individuals carrying the progenitor nonrearranged chromosome *A12*. The detected cases of gene upregulation in *A4* could be explained by taking into account the reported ability of HP1a not only to repress but also to activate individual genes (Cryderman *et al.* 2005; De Lucia *et al.* 2005; Hediger and Gasser 2006; de Wit *et al.* 2007; Cryderman *et al.* 2011; Eissenberg and Elgin 2014).

We found that the heterochromatin effect on a given gene in *A4* depends on the developmental stage because all the genes demonstrating repression or activation in third instar larvae showed no significant expression changes in adults. This observation may be explained by assuming that the heterochromatinization perturbs not the transcription itself but the changes in gene transcription state (either activation or

repression), which are, in turn, coupled with chromatin remodeling. The late larval stage is the period when a vast number of genes change their transcription state and presumably become sensitive to heterochromatin influence.

The *A4* inversion is able to induce *trans*-inactivation of reporter transgenes on the homologous chromosome. This ability was shown primarily by the observation of variegated eye phenotype in *A12/A4* flies (Figure 1C). *trans*-Inactivation caused by *A4* was probed using the *mini-white*-containing transgenes located on the normal chromosome 2 in the regions that are homologous to the *A4* regions adjacent to heterochromatin. *trans*-Inactivation spreads over an area of 475 kb from the main satellite block (up to transgene 19883) (Figure 3, region E) and over an area of 40 kb (Figure 3, region A) from the small, detached heterochromatic block.

Inactivation of transgenes on the normal chromosome in combination with *A4* is continuous both in the 40-kb area adjacent to the main block of pericentromeric heterochromatin and near the small, detached heterochromatic block (Figure 3, regions A and B). All types of transgenes inserted into promoters and coding and intergenic regions undergo inactivation. The single exception in this region is the noninactivated 10662 (*P[lacW]*) transgene inserted into the 5' UTR of the *CG9246* gene 18.6 kb from the small, detached block of heterochromatin. The presence of a GAGA factor binding site in *P[EP]* and *P[EPgy2]* transgenes or the *Su(Hw)* binding site in *PBac[WH]* genes does not prevent repression. These sites demonstrate insulator properties, but it seems that two

copies should flank the reporter gene to obtain effective protection from inactivation.

The region ~80 kb in size (Figure 3, region C) demonstrates interspersed *trans*-inactivation. Closely located transgene pairs with different responses to inactivation are represented by *SH0764* (*P[lacW]*)/*11019* (*P[lacW]*) and *20102* (*P[EPgy2]*)/*12400* (*P[GT1]*). The first pair lies in the 5' UTR of the *CG8671* gene, and the insertions are separated by 326 bp. Transgene *SH0764* but not *11019* is sensitive to *trans*-inactivation, and both are of the same type, *P[lacW]*. In the second pair of transgenes separated by 500 bp, *20102* is not *trans*-inactivated, while *12400* is moderately inactivated. Transgene *20102* is inserted upstream of the *crc* gene, and *12400* is in its 5' UTR.

We revealed different responses to *trans*-inactivation of transgenes separated by only 9 bp (*10662* and *EP2348* in the 5' UTR of the *CG9246* gene) (Figure 3, region A), which raises the question of whether chromatin organization at the insertion site is a determining factor of *trans*-inactivation. Rather, the differences in *trans*-inactivation of closely located transgenes can be explained by the formation of individual chromatin structures including functional elements of the transgene and its target in each case of insertion.

The effects of *cis*- and *trans*-inactivation of heterochromatin on the homologous regions on the rearranged and normal chromosomes do not follow each other (Figure 2 and Figure 3). Euchromatic genes in their natural environment appear to be quite resistant to heterochromatin influence, presumably because of the presence of full sets of regulatory elements (*i.e.*, enhancers, insulators, etc.). Just a few genes near the euchromatin-heterochromatin border in the *A4* chromosome are affected, while the inactivation of transgenes on the homologous chromosome is strong and can be detected far from heterochromatin. Transgenes containing *mini-white* reporters are quite sensitive to repression when placed into a heterochromatin environment [this work, the *bw^D* example, and earlier observations such as those of Martin-Morris *et al.* (1997)], presumably because of the lack of a full set of regulatory elements.

Transgenes in the same region (*e.g.*, the abovementioned *11127* and *20102*) (Figure 3, region C) can be inactivated or not, respectively, and we suppose that heterochromatin formation proceeds autonomously on a transgene dragged into the heterochromatic compartment and may induce heterochromatinization on the homologous rearranged chromosome, an initiator of the dragging of the heterochromatic compartment, and subsequent *trans*-inactivation (Figure 4).

An additional observation pointing to different mechanisms of *cis*- and *trans*-inactivation is the existence of mutations specifically affecting *trans*- but not *cis*-inactivation in *A4*. We showed that two chromatin-related proteins, SAYP and AGO2, act as potent noncanonic PEV modifiers of *trans*-inactivation. SAYP protein, a subunit of the *SWI/SNF* complex (Chalkley *et al.* 2008) has been characterized as a chromatin coactivator (Shidlovskii *et al.* 2005). At the same time, SAYP binds to heterochromatin, and its deficiency suppresses

heterochromatin-induced repression of transgenes and the *white* gene in the *w^{m4h}* inversion (Shidlovskii *et al.* 2005). In our case, *SAYP* mutation strongly suppresses *trans*-inactivation but not *cis*-repression of transgenes in *A4* (Figure 6). *AGO2* mutations, by contrast, enhance *trans*-inactivation but just slightly affect *cis*-repression of transgene in *A4* (Figure 6). Apart from its role in siRNA-based RNA interference (RNAi), AGO2 is considered to be a component of active chromatin in *Drosophila* (Cernilogar *et al.* 2011) and an insulator-associated protein (Cernilogar *et al.* 2011; Moshkovich *et al.* 2011). Although the exact mechanisms of the opposite effects of *AGO2* and *SAYP* mutations on *trans*-inactivation remain obscure, it is possible that SAYP directly participates in the heterochromatinization *de novo*, while AGO2 is necessary for the proper functioning of insulators around the *trans*-inactivated reporter gene.

trans-Inactivation caused by *A4* shows similarities to the earlier-studied ability of the *bw^D* allele to silence the homologous *bw* allele and the *mini-white*-containing transgenes *in trans*. Up to the present, *bw^D* was essentially unique and the most extensively explored example of PEV-induced *trans*-inactivation in the fruit fly. *bw^D* was caused by insertion of the AAGAG satellite (1.6 Mb) into the coding sequence of the *brown* gene (Sage *et al.* 2005). It was expected and then experimentally confirmed that the presence of somatic pairing of the homologous chromosome in *Drosophila* and the ability of heterochromatic repeated regions to stick together underlie the dragging of euchromatin into the heterochromatic compartment by the *bw^D* allele (Csink and Henikoff 1996, 1998; Fung *et al.* 1998; Thakar and Csink 2005). The molecular mechanism of heterochromatin formation in *trans*-inactivation differs from its *cis*-spreading because it is independent of the histone methyltransferase SU(VAR)3-9 (Nisha *et al.* 2008). In the case of *bw^D* *trans*-inactivation, deletion mapping (Sage *et al.* 2005) identified the 301-bp region acting as an enhancer of *trans*-inactivation; it contained multiple binding sites for BEAF insulator protein and was enriched by BEAF (according to the ChIP chip profile modENCODE). However, we found no obvious correlations between BEAF enrichment and transgene inactivation sites using the modENCODE BEAF profile.

We found no *trans*-inactivation of transgenes in the region immediately proximal to the histone gene cluster (Figure 3, region D), while it occurred further away from both sides of the cluster. Since *A4*, like *bw^D*, causes dragging of euchromatic regions into the heterochromatic compartment (Abramov *et al.* 2011; Lavrov *et al.* 2013), we checked whether a distinct intranuclear placement of the histone gene cluster may be responsible for the suppression of *trans*-inactivation. 3D confocal imaging using probes for the *trans*-inactivated region and the histone gene cluster shows that the latter forms a distinct subcompartment located on the border of the heterochromatic compartment but outside of it (Figure 5). We assume that this is the reason for the large-scale gap in *trans*-inactivation spreading near the histone gene cluster.

Studies of the genetic system described herein allow us to consider *cis*- and *trans*-inactivation driven by chromosomal rearrangement as two relatively independent processes of heterochromatinization. We showed no correlation between *cis*-repression of genes near the euchromatin-heterochromatin border and inactivation of transgenes on a homologous chromosome (Figure 2 and Figure 3). The process of transgene heterochromatinization seems to be independent of *cis*-spreading of heterochromatin because the binding of HP1a to the transgene occurs in the absence of HP1a at the homologous site on the rearranged A4 chromosome. The detection of genes specifically affecting the *trans*-inactivation process also points to different mechanisms of *cis*-repression and transgene inactivation.

Acknowledgments

We are grateful to M. Logacheva (A. Kondrashov Group at Moscow State University) for performing NGS runs and to Yu. Shevelyov for helpful discussion. Stocks obtained from the Bloomington *Drosophila* Stock Center (National Institutes of Health P40-OD018537) were used in this study. This work was supported by grants from the Russian Foundation for Basic Research (13-04-40138 to V.A.G. and 14-04-32308 to A.S.Sh.) and the Molecular and Cell Biology Program of the Russian Academy of Sciences (to V.A.G.).

Literature Cited

- Abramov, Y. A., M. V. Kibanov, V. A. Gvozdev, and S. A. Lavrov, 2011 Genetic and molecular analysis of gene trans-inactivation caused by homologous eu-heterochromatic chromosome rearrangement in *Drosophila melanogaster*. *Dokl. Biochem. Biophys.* 437: 72–76.
- Cernilogar, F. M., M. C. Onorati, G. O. Kothe, A. M. Burroughs, K. M. Parsi *et al.*, 2011 Chromatin-associated RNA interference components contribute to transcriptional regulation in *Drosophila*. *Nature* 480: 391–395.
- Chalkley, G. E., Y. M. Moshkin, K. Langenberg, K. Bezstarosti, A. Blastyak *et al.*, 2008 The transcriptional coactivator SAYP is a trithorax group signature subunit of the PBAP chromatin remodeling complex. *Mol. Cell. Biol.* 28: 2920–2929.
- Cryderman, D. E., S. K. Grade, Y. Li, L. Fanti, S. Pimpinelli *et al.*, 2005 Role of *Drosophila* HP1 in euchromatic gene expression. *Dev. Dyn.* 232: 767–774.
- Cryderman, D. E., M. W. Vitalini, and L. L. Wallrath, 2011 Heterochromatin protein 1a is required for an open chromatin structure. *Transcription* 2: 95–99.
- Csink, A. K., and S. Henikoff, 1996 Genetic modification of heterochromatic association and nuclear organization in *Drosophila*. *Nature* 381: 529–531.
- Csink, A. K., and S. Henikoff, 1998 Large-scale chromosomal movements during interphase progression in *Drosophila*. *J. Cell Biol.* 143: 13–22.
- De Lucia, F., J. Q. Ni, C. Vaillant, and F. L. Sun, 2005 HP1 modulates the transcription of cell-cycle regulators in *Drosophila melanogaster*. *Nucleic Acids Res.* 33: 2852–2858.
- de Wit, E., F. Greil, and B. van Steensel, 2007 High-resolution mapping reveals links of HP1 with active and inactive chromatin components. *PLoS Genet.* 3: e38.
- Dimitri, P., 1991 Cytogenetic analysis of the second chromosome heterochromatin of *Drosophila melanogaster*. *Genetics* 127: 553–564.
- Eberl, D. F., L. J. Lorenz, M. B. Melnick, V. Sood, P. Lasko *et al.*, 1997 A new enhancer of position-effect variegation in *Drosophila melanogaster* encodes a putative RNA helicase that binds chromosomes and is regulated by the cell cycle. *Genetics* 146: 951–963.
- Eissenberg, J. C., and S. C. Elgin, 2014 HP1a: a structural chromosomal protein regulating transcription. *Trends Genet.* 30: 103–110.
- Elgin, S. C., and G. Reuter, 2013 Position-effect variegation, heterochromatin formation, and gene silencing in *Drosophila*. *Cold Spring Harb. Perspect. Biol.* 5: a017780.
- Fung, J. C., W. F. Marshall, A. Dernburg, D. A. Agard, and J. W. Sedat, 1998 Homologous chromosome pairing in *Drosophila melanogaster* proceeds through multiple independent initiations. *J. Cell Biol.* 141: 5–20.
- Gatti, M., S. Bonaccorsi, and S. Pimpinelli, 1994 Looking at *Drosophila* mitotic chromosomes. *Methods Cell Biol.* 44: 371–391.
- Grewal, S. I., and S. C. Elgin, 2002 Heterochromatin: new possibilities for the inheritance of structure. *Curr. Opin. Genet. Dev.* 12: 178–187.
- Hazlerigg, T., and S. Petersen, 1992 An unusual genomic position effect on *Drosophila* white gene expression: pairing dependence, interactions with zeste, and molecular analysis of revertants. *Genetics* 130: 125–138.
- Hediger, F., and S. M. Gasser, 2006 Heterochromatin protein 1: don't judge the book by its cover! *Curr. Opin. Genet. Dev.* 16: 143–150.
- Hines, K. A., D. E. Cryderman, K. M. Flannery, H. Yang, M. W. Vitalini *et al.*, 2009 Domains of heterochromatin protein 1 required for *Drosophila melanogaster* heterochromatin spreading. *Genetics* 182: 967–977.
- Klenov, M. S., S. A. Lavrov, A. D. Stolyarenko, S. S. Ryazansky, A. A. Aravin *et al.*, 2007 Repeat-associated siRNAs cause chromatin silencing of retrotransposons in the *Drosophila melanogaster* germline. *Nucleic Acids Res.* 35: 5430–5438.
- Lavrov, S. A., A. S. Shatskikh, M. V. Kibanov, and V. A. Gvozdev, 2013 Correlation on a cellular level of gene transcriptional silencing and heterochromatin compartment dragging in case of PEV-producing eu-heterochromatin rearrangement in *Drosophila melanogaster*. *Mol. Biol.* 47: 286–291 (in Russian).
- Lohe, A. R., A. J. Hilliker, and P. A. Roberts, 1993 Mapping simple repeated DNA sequences in heterochromatin of *Drosophila melanogaster*. *Genetics* 134: 1149–1174.
- Martin-Morris, L. E., A. K. Csink, D. R. Dorer, P. B. Talbert, and S. Henikoff, 1997 Heterochromatic trans-inactivation of *Drosophila* white transgenes. *Genetics* 147: 671–677.
- Moshkovich, N., P. Nisha, P. J. Boyle, B. A. Thompson, R. K. Dale *et al.*, 2011 RNAi-independent role for Argonaute2 in CTCF/CP190 chromatin insulator function. *Genes Dev.* 25: 1686–1701.
- Nisha, P., J. L. Plank, and A. K. Csink, 2008 Analysis of chromatin structure of genes silenced by heterochromatin in trans. *Genetics* 179: 359–373.
- Pal-Bhadra, M., B. A. Leibovitch, S. G. Gandhi, M. Rao, U. Bhadra *et al.*, 2004 Heterochromatic silencing and HP1 localization in *Drosophila* are dependent on the RNAi machinery. *Science* 303: 669–672.
- Sage, B. T., J. L. Jones, A. L. Holmes, M. D. Wu, and A. K. Csink, 2005 Sequence elements in cis influence heterochromatic silencing in trans. *Mol. Cell. Biol.* 25: 377–388.
- Schotta, G., A. Ebert, V. Krauss, A. Fischer, J. Hoffmann *et al.*, 2002 Central role of *Drosophila* SU(VAR)3-9 in histone H3-K9 methylation and heterochromatic gene silencing. *EMBO J.* 21: 1121–1131.

- Schotta, G., A. Ebert, and G. Reuter, 2003 SU(VAR)3-9 is a conserved key function in heterochromatic gene silencing. *Genetica* 117: 149–158.
- Shidlovskii, Y. V., A. N. Krasnov, J. V. Nikolenko, L. A. Lebedeva, M. Kopantseva *et al.*, 2005 A novel multidomain transcription co-activator SAYP can also repress transcription in heterochromatin. *EMBO J.* 24: 97–107.
- Shpiz, S., S. Lavrov, and A. Kalmykova, 2014 Combined RNA/DNA fluorescence in situ hybridization on whole-mount *Drosophila* ovaries. *Methods Mol. Biol.* 1093: 161–169.
- Spofford, J. B., 1976 Position-effect variegation in *Drosophila*, pp. 955–1018 in *The Genetics and Biology of Drosophila*, M. Ashburner, and E. Novitski, eds. Academic Press, New York.
- Talbert, P. B., and S. Henikoff, 2006 Spreading of silent chromatin: inaction at a distance. *Nat. Rev. Genet.* 7: 793–803.
- Thakar, R., and A. K. Csink, 2005 Changing chromatin dynamics and nuclear organization during differentiation in *Drosophila* larval tissue. *J. Cell Sci.* 118: 951–960.
- Tulin, A. V., N. M. Naumova, A. A. Aravin, and V. A. Gvozdev, 1998 Repeated, protein-encoding heterochromatic genes cause inactivation of a juxtaposed euchromatic gene. *FEBS Lett.* 425: 513–516.
- Vogel, M. J., L. Pagie, W. Talhout, M. Nieuwland, R. M. Kerkhoven *et al.*, 2009 High-resolution mapping of heterochromatin redistribution in a *Drosophila* position-effect variegation model. *Epigenet. Chromatin* 2: 1.

Communicating editor: J. A. Birchler

GENETICS

Supporting Information

www.genetics.org/lookup/suppl/doi:10.1534/genetics.115.181693/-/DC1

The Differences Between *Cis*- and *Trans*-Gene Inactivation Caused by Heterochromatin in *Drosophila*

Yuriy A. Abramov, Aleksei S. Shatskikh, Oksana G. Maksimenko, Silvia Bonaccorsi, Vladimir A. Gvozdev, and Sergey A. Lavrov

Table S1

List of transgene-bearing fly lines used for trans-inactivation checks and brief description of transgenes used.

Table S2

List of primers and synthetic DNA fragments used in this study.

Table S3

RNA-seq and qPCR numeric data for the genes mentioned in the manuscript.

Table S4

List of genes and their alleles tested for the effects on cis- and trans-inactivation.

Table S5

Comparison of expression levels of genes near the A4 breakpoint in wild-type larvae and the degree of cis-inactivation of these genes in A4/A4 larvae.

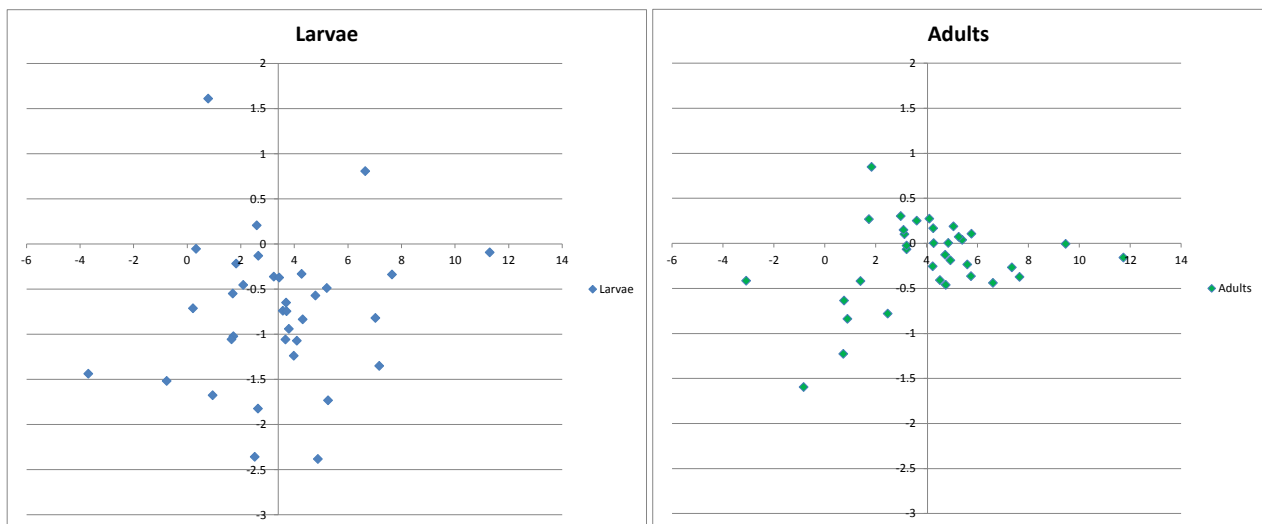
Stock number	INSERTED ELEMENT	Trans-inactivation	DIST FROM BP	Position	LOCATION STRAND	INSERTED ELEMENT SIZE	AFFECTED GENES	FBID	STOCK
12451	P(GT1)	No	-532024	chr2L:20650190-20650191	1	8.447	CG2611	FBH0017194	12451 w[1118]: P(GT1)CG2611[BG00938]
12591	P(GT1)	No	-329676	chr2L:20852538-20852539	1	8.447	CG9335	FBH0017668	12591 w[1118]: P(GT1)BG01978
12406	P(GT1)	No	-264337	chr2L:20917877-20917878	-1	8.447	Atg9	FBH0017147	12406 w[1118]: P(GT1)dy[BG00162]
15527	P(EFpgy2)	No	-211282	chr2L:20970932-20970933	1	10.908	CG9266	FBH0027093	15527 y[1] w[67c23]; P(EFpgy2)CG42238[EY01654]
16715	P(EFpgy2)	No	-196068	chr2L:20986146-20986147	1	10.908	CG42238	FBH0039322	16715 y[1] w[67c23]; P(EFpgy2)CG42238[EY06338]
16113	PBac(SHPw+1)	No	-168014	chr2L:21014191-21014201	1	6.938	CG42238	FBH0037689	16113 y[1] w[1118]: PBac(SHPw+1)CG42238[A428]/CyO
20390	P(wHy)	No	-130760	chr2L:21051454-21051455	1	15.588	CG42238	FBH0072674	20390 y[1] w[67c23]; P(wHy)CG42238[DG04612]
12532	P(GT1)	No	-129214	chr2L:21053000-21053001	1	8.447	betainH-nu	FBH0018406	12532 w[1118]: P(GT1)betainH-nu[BG01037]
19146	P(wHy)	No	-112170	chr2L:21070044-21070045	1	7.303	CG9265	FBH0042742	19146 w[1118]: P(wHy)CG9265[K00590]
19930	P(EFpgy2)	No	-79479	chr2L:21102735-21102736	1	10.908	-	FBH0039942	19930 y[1] w[67c23]; P(EFpgy2)EY08505
20292	P(EFpgy2)	No	-73675	chr2L:21108539-21108540	1	10.908	Nhe2	FBH0040222	20292 y[1] w[67c23]; P(EFpgy2)Nhe2[EY11323]
19582	P(EF)	Yes++	-40312	chr2L:21141902-21141903	-1	7.987	Dap160	FBH0011223	19582 w[1118]: P(EF)Dap160[EP2543]
SH0471	P(lacW)	Yes+++	-38603	chr2L:21143267-21143612	-	10.691	I(2)SH0471	FBH0026226	-
19661	P(EFpgy2)	Yes+++	-38047	chr2L:21143267-21143268	1	10.908	CG9253	FBH0039673	19661 y[1] w[67c23]; P(EFpgy2)CG9253[EY02880]/CyO
18010	PBac(RB)	Yes++	-34702	chr2L:21147512-21147513	-1	5.971	del	FBH0041560	18010 w[1118]: PBac(RB)del[402039]/CyO
SH2164	P(lacW)	Yes+++	-33283	chr2L:21148427-21148932	-	10.691	I(2)SH2164	FBH0025696	-
SH0354	P(lacW)	Yes++	-25866	chr2L:21156176-21156349	-	10.691	I(2)SH0354	FBH0026288	-
17314	P(EFpgy2)	Yes+++	-25978	chr2L:21156236-21156237	-1	10.908	E2f2	FBH0038690	17314 y[1] w[67c23]; P(EFpgy2)E2f2[EY02995]
5229_1	P(lacW)	Yes+++	-25316	chr2L:21156898-21156899	-	10.691	Myp6	FBH0033471	5229 y[1] w[67c23]; P(lacW)Myp6[K16403]/CyO
18383	PBac(WH)	Yes++	-23565	chr2L:21158649-21158650	1	7.234	CG9249	FBH0041950	18383 w[1118]: PBac(WH)CG9249[F00877]
18375	PBac(WH)	Yes++	-23562	chr2L:21158652-21158653	-1	7.234	CG9249	FBH0041942	18375 w[1118]: PBac(WH)CG9249[F00835]/CyO
SH2113	P(lacW)	Yes+++	-19202	chr2L:21162912-21163013	-	10.691	I(2)SH2113	FBH0025712	-
16587	P(EFpgy2)	Yes++	-19191	chr2L:21163023-21163024	-1	10.908	CG9247	FBH0039166	16587 y[1] w[67c23]; P(EFpgy2)CG9247[EY04057]
10662	P(lacW)	No	-18553	chr2L:21163661-21163662	1	10.691	I(2)K07215	FBH0006703	10662 y[1] w[67c23]; P(lacW)Myp6[K16403]/CyO
EP2348	P(EF)	Yes++	-18545	chr2L:21163669-21163670	-1	7.987	CG9246	FBH0016413	-
SH0608	P(lacW)	Yes+++	-13277	chr2L:21168651-21168938	-	10.691	Acon	FBH0025168	-
20708	P(EFpgy2)	Yes+++	-13551	chr2L:21168663-21168664	-	10.908	Acon	FBH0057677	20708 y[1] w[67c23]; P(EFpgy2)Acon[EY11898]/CyO
20250	P(EFpgy2)	Yes++	-2567	chr2L:21179647-21179648	-1	10.908	bur	FBH0040180	20250 y[1] w[67c23]; P(EFpgy2)bur[EY11080]/CyO
43099	Mi(MIC)	Yes+++	12958	chr2L:21195076-21195077	-1	7.267	Ret	FBH0150551	43099 y[1] w[1]; Mi(Y+miDm2)-MICRet[MiO7200]/SM6a
20229	P(EFpgy2)	Yes+++	23569	chr2L:21205783-21205784	-1	10.908	-	FBH0040159	20229 y[1] w[67c23]; P(EFpgy2)EY10934
19922	P(EFpgy2)	Yes+++	24119	chr2L:21206133-21206134	1	10.908	-	FBH0039934	19922 y[1] w[67c23]; P(EFpgy2)EY07947/CyO
20872	P(EFpgy2)	Yes+++	24168	chr2L:21206382-21206383	-	10.908	-	FBH0057845	20872 y[1] w[67c23]; P(EFpgy2)EY13357
10879	P(lacW)	Yes+++	32953	chr2L:21215167-21215168	1	10.691	snRNA-U4-398	FBH0006577	10879 y[1] w[67c23]; P(lacW)snRNA-U4-398[K09410]/CyO
20175	P(EFpgy2)	Yes+++	39066	chr2L:21221280-21221281	1	10.908	-	FBH0040078	20175 y[1] w[67c23]; P(EFpgy2)EY08386
SH0778	P(lacW)	Yes+++	39751	chr2L:21221701-21221966	-	10.691	CG8677	FBH0026091	-
EP988	P(EF)	Yes++	39814	chr2L:21222028-21222029	-	7.987	CG8677	FBH0010729	-
20152	P(EFpgy2)	TransActivation	55057	chr2L:21232721-21232722	1	10.908	Hr39	FBH0040055	20152 y[1] w[67c23]; P(EFpgy2)Hr39[EY04579]
55A12	P(w-65te) Hr39	TransActivation	55064	chr2L:21232728-21232729	-1	-	Hr39	-	-
EP2490	P(EF)	TransActivation	55621	chr2L:21237835-21237836	1	7.987	Hr39	FBH0011178	-
DHR39	P(lacW)	No	71339	chr2L:21238567-21235554	1	10.691	EcoI/lacZ	FBH0007257	-
12679	P(GT1)	No	68555	chr2L:21250769-21250770	1	8.447	Hr39	FBH0017714	12679 w[1118]: P(GT1)Hr39[BG02396]
EP2507	P(EF)	No	68583	chr2L:21250797-21250798	-1	7.987	Hr39	FBH0021114	-
11127	P(lacW)	Yes+++	79006	chr2L:21261220-21261221	1	10.691	I(2)K14505	FBH0006409	11127 y[1] w[67c23]; P(lacW)I(2)K14505[K14505]/CyO
19694	P(EFpgy2)	Yes+++	79335	chr2L:21261549-21261550	1	10.908	I(2)K14505	FBH0039706	19694 y[1] w[67c23]; P(EFpgy2)I(2)K14505[EY04514]/CyO
SH0764	P(lacW)	Yes++	80830	chr2L:21262995-21263045	-	10.691	I(2)SH0764	FBH0026097	-
11019	P(lacW)	No	81125	chr2L:21263339-21263340	1	10.691	I(2)K11226	FBH0006484	11019 y[1] w[67c23]; P(lacW)I(2)K11226[K11226]/CyO
10562	P(lacW)	Yes+++	113681	chr2L:21295895-21295896	1	10.691	I(2)K05106	FBH0006819	10562 y[1] w[67c23]; P(lacW)I(2)K05106[K05106]/CyO
20102	P(EFpgy2)	No	127336	chr2L:21309750-21309751	1	10.908	Mlu	FBH0040005	20102 y[1] w[67c23]; P(EFpgy2)Mlu[EY00908]
12400	P(GT1)	Yes+	128691	chr2L:21310905-21310906	-1	8.447	crc	FBH0017141	12400 w[1118]: P(GT1)crc[BG00047]
21396	P(EFpgy2)	No	136809	chr2L:21319023-21319024	1	10.908	crc	FBH0057990	21396 y[1] w[67c23]; P(EFpgy2)crc[EY12903]
21432	P(EFpgy2)	No	157052	chr2L:21339266-21339267	1	10.908	dimm	FBH0058026	21432 y[1] w[67c23]; P(EFpgy2)dimm[EY14636]
16407	P(EFpgy2)	No	161687	chr2L:21343901-21343902	1	10.908	-	FBH0039425	16407 y[1] w[67c23]; P(EFpgy2)EY07263
12761	P(GT1)	No	197953	chr2L:21380167-21380168	1	8.447	inv3	FBH0115741	12761 w[1118]: P(GT1)inv3[BG01341]
20886	P(EFpgy2)	Yes+	426567	chr2L:21608781-21608782	1	10.908	-	FBH0057859	20886 y[1] w[67c23]; P(EFpgy2)EY13580
SH2339	P(lacW)	Yes+	442074	chr2L:21624116-21624289	-	10.691	Cul-2	FBH0025648	-
10579	P(lacW)	Yes+	447107	chr2L:21629321-21629322	1	10.691	Df31	FBH0006768	10579 y[1] w[67c23]; P(lacW)Df31[K05815]/CyO
20104	P(EFpgy2)	Yes++	447798	chr2L:21630012-21630013	-1	10.908	-	FBH0040007	20104 y[1] w[67c23]; P(EFpgy2)EY00951
15680	P(EFpgy2)	Yes++	450359	chr2L:21632573-21632574	-1	10.908	-	FBH0027253	15680 y[1] w[67c23]; P(EFpgy2)EY03638
20063	P(EFpgy2)	Yes++	451189	chr2L:21633403-21633404	1	10.908	Ac3	FBH0039815	20063 y[1] w[67c23]; P(EFpgy2)Ac3[EY10141]
12762	P(GT1)	Yes+++	470980	chr2L:21653194-21653195	1	8.447	-	FBH0018088	12762 w[1118]: P(GT1)BG01382
19883	P(EFpgy2)	Yes++	476805	chr2L:21659019-21659020	1	10.908	Cul-2	FBH0039895	19883 y[1] w[67c23]; P(EFpgy2)Cul-2[EY09124]
20683	P(EFpgy2)	No	495077	chr2L:21677291-21677292	-1	10.908	CG2225	FBH0057650	20683 y[1] w[67c23]; P(EFpgy2)CG2225[EY11545]
20499	P(wHy)	No	495702	chr2L:21677916-21677917	1	15.588	-	FBH0072810	20499 y[1] w[67c23]; P(wHy)DG29208/SM6a
10770	P(lacW)	No	574612	chr2L:21755826-21755827	1	10.691	step	FBH0006650	10770 y[1] w[67c23]; P(lacW)step[K01110]/CyO
11178	P(lacW)	No	646275	chr2L:21828489-21828490	1	10.691	I(2)K16406	FBH0006360	11178 y[1] w[67c23]; P(lacW)I(2)K16406[K16406]/CyO
18789	PBac(WH)	No	732242	chr2L:21914456-21914457	1	7.234	CG31600	FBH0042372	18789 w[1118]: PBac(WH)CG31600[F04602]
17367	P(EFpgy2)	No	934521	chr2L:22116735-22116736	1	10.908	-	FBH0038737	17367 y[1] w[67c23]; P(EFpgy2)EY06734
15021	P(EFpgy2)	No	949197	chr2L:22131411-22131412	1	10.908	CycK	FBH0024854	15021 y[1] w[67c23]; P(EFpgy2)EY00324
16093	PBac(SHPw+1)	No	977964	chr2L:22160178-22160179	-1	6.938	-	FBH0037869	16093 y[1] w[1118]: PBac(SHPw+1)A317

P-element mediated insertions with mini-white reporter used for trans-inactivation analysis

Transgene	Number of checked(inactivated) insertions	Comment
P(lacW)	18(13)	Hsp70 promoter- mini-white and P-transposase- LacZ fusion, construction works as enhancer trap
P(EF)	5(4)	mini-white and combination of Trl binding sites, UAS and Hsp70 promoter to allow inducible misexpression of gene in element insertion point
P(EFpgy2)	27(16)	like P(EF) but contains also yellow gene
PBac(RB)	1(1)	piggyBack based construction with mini-white , FRT site and splice acceptor site (exon from Rbp1)
PBac(WH)	3(2)	piggyBack based construction with mini-white , FRT site, UAS at one end and insulator (Su(Hw) binding site) at opposite end
P(GT1)	8(2)	contains promoter-less GAL4 gene, neofix gene under Hsp70 promoter and mini-white containing splicing donor site instead of polyadenylation signal
P(wHy)	2(0)	Element for generation of deletions, contains mini-white , yellow and bobo mobile element
PBac(SHPw+1)	2(0)	piggyBack based construction with mini-white
P(XP)	1(0)	mini-white , FRT sites flanking UAS, two UAS at both ends and insulator (Su(Hw) binding site)

Chr	Start	End	tracking_id	Strand	A12L FPKM	A12A FPKM	log2(A12)L	Log2(A4/A12)L	log2(A12)A	Log2(A4/A12)A
chr2L	21102742	21104321	CG9257	+	12.98	19.40	3.70	-0.65	4.28	0.00
chr2L	21104567	21134255	Nhe2	+	17.13	9.29	4.10	-1.07	3.22	-0.07
chr2L	21134438	21142353	Dap160	-	15.82	12.24	3.98	-1.24	3.61	0.25
chr2L	21143228	21145146	CG9253	+	6.30	17.26	2.66	-0.13	4.11	0.27
chr2L	21154292	21156232	E2f2	-	11.93	33.37	3.58	-0.74	5.06	0.19
chr2L	21156873	21157685	Mpp6	+	3.26	9.31	1.70	-0.55	3.22	-0.03
chr2L	21157432	21158588	CG9249	-	6.06	23.05	2.60	0.21	4.53	-0.41
chr2L	21158877	21160783	CG9248	+	37.13	26.59	5.21	-0.49	4.73	-0.13
chr2L	21160635	21163087	Nbr	-	13.13	48.58	3.71	-0.75	5.60	-0.23
chr2L	21163610	21166090	CG9246	+	9.41	42.32	3.23	-0.36	5.40	0.04
chr2L	21166045	21168344	CG43345	-	4.28	7.93	2.10	-0.45	2.99	0.30
chr2L	21168615	21173017	Acon	+	100.40	705.57	6.65	0.81	9.46	-0.01
chr2L	21174382	21179697	bur	-	27.68	54.41	4.79	-0.57	5.77	0.10
chr2L	21212321	21220572	CG8678	-	38.33	8.77	5.26	-1.73	3.13	0.10
chr2L	21216003	21218544	CG8679	-	6.27	8.56	2.65	-1.82	3.10	0.15
chr2L	21221311	21231694	CG8677	+	3.31	3.58	1.72	-1.02	1.84	0.85
chr2L	21237249	21259675	Hr39	+	5.76	1.86	2.53	-2.36	0.90	-0.84
chr2L	21261167	21262411	l(2)k14505	+	19.36	38.38	4.28	-0.33	5.26	0.07
chr2L	21262955	21282514	CG8671	+	13.91	18.91	3.80	-0.94	4.24	-0.26
chr2L	21286077	21310050	Mio	+	10.85	19.19	3.44	-0.37	4.26	0.17
chr2L	21310853	21319527	crc	+	200.70	163.78	7.65	-0.34	7.36	-0.27
chr2L	21344606	21358271	Tsp39D	+	3.15	5.56	1.66	-1.06	2.48	-0.78
chr2L	21371226	21377995	CG8665	+	1.73	2.65	0.79	1.61	1.41	-0.42
chr2L	21379999	21393319	nrv3	+	3.56	27.07	1.83	-0.22	4.76	-0.46
chr2L	21573388	21577103	Lamp1	+	130.47	97.52	7.03	-0.82	6.61	-0.44
chr2L	21578318	21589355	nompB	-	0.08	0.12	-3.69	-1.44	-3.09	-0.42
chr2L	21614231	21623627	CG2201	-	29.55	53.73	4.89	-2.38	5.75	-0.37
chr2L	21624678	21626190	CR43148	+	0.59	0.56	-0.76	-1.52	-0.83	-1.60
chr2L	21626308	21629932	Df31	-	144.26	201.25	7.17	-1.35	7.65	-0.37
chr2L	21632586	21647964	Ac3	+	1.16	1.69	0.22	-0.71	0.76	-0.64
chr2L	21658734	21663698	Cul-2	+	19.90	30.63	4.32	-0.83	4.94	-0.19
chr2L	21663805	21677530	CG2225	-	1.94	1.66	0.95	-1.68	0.73	-1.23
chr2L	21678049	21682116	Ef2b	-	2514.29	3413.46	11.30	-0.09	11.74	-0.16
chr2L	21684102	21729051	CG31619	+	1.26	3.34	0.33	-0.05	1.74	0.27
chr2L	21740040	21757466	step	-	12.73	28.94	3.67	-1.06	4.86	0.00

Scatterplots of log2-transformed ratios of A4 to A12 expression levels (Y axis) ver. log2-transformed FPKMs in A12 (X axis) larvae and adults for genes near the A4 eu-heterochromatin border. There is no obvious correlation between the expression level of the gene and its sensitivity to cis-inactivation by heterochromatin



Gene	Synonym	Allele checked	Allele nature	Gene product function	Effect of mutation on trans-inactivation	Effect of mutation on cis-inactivation
Chromosome X						
<i>e(y)3</i>	<i>SAYP</i>	<i>e(y)3⁴ (e(y)3^{u1})</i>	<i>Stalker insertion, truncated protein</i>	Chromatin binding, chromatin remodeling, heterochromatin establishment on chromosome 4	very strong suppression	no effect
<i>zeste</i>		<i>z¹</i>	<i>Gain of function, point mutation</i>	Chromatin binding, transvection	no effect	no effect
Chromosome 2						
<i>Su(var)2-5</i>	<i>CG8409</i>	<i>Su(var)2-5¹</i>	<i>EMS, loss of function</i>	HP1a chromodomain protein	very strong suppression	very strong suppression
<i>UAP56</i>	<i>HEL</i>	<i>sz¹⁵ /uap56²⁸</i>	<i>hypomorphic</i>	mRNA nuclear transport	no effect	no effect
<i>eggless</i>	<i>dSETDB1</i>	<i>egg¹⁴⁷³</i>	<i>EMS, truncated protein</i>	H3-K9 specific histone methyltransferase activity	strong suppression	strong suppression
<i>piwi</i>	<i>CG6122</i>	<i>piwi² /powi^{NT}</i>	<i>hypomorphic</i>	piRNA binding, transposon silencing	no effect	no effect
Chromosome 3						
<i>Su(var)3-1</i>	<i>JIL-1</i>	<i>JIL-1¹</i>	<i>EMS, gain of function</i>	histone kinase activity (H3-S10 specific), prevents heterochromatin spreading	medium suppression	strong suppression
<i>Su(var)3-6</i>	<i>Pp1-87B</i>	<i>Su(var)3-6⁰¹</i>	<i>EMS, hypomorphic</i>	Catalytic subunit of PP1 protein phosphatase. Regulates chromosome condensation and affects mitotic chromosome segregation	strong suppression	strong suppression
<i>Su(var)3-7</i>	<i>CG8599</i>	<i>Su(var)3-7^{0f}</i>	<i>Delta2-3 EMS</i>	DNA binding C2H2-like Zinc finger protein	very strong suppression	strong suppression
<i>Su(var)3-7</i>	<i>CG8599</i>	<i>Su(var)3-7^{p12}</i>			very strong suppression	strong suppression
<i>Su(var)3-7</i>	<i>CG8599</i>	<i>Su(var)3-7^{p43}</i>			very strong suppression	strong suppression
<i>Su(var)3-9</i>	<i>CG43664</i>	<i>Su(var)3-9¹</i>	<i>EMS, loss of function EMS, X ray EMS, hypomorphic hypomorphic</i>	H3-K9 specific histone methyltransferase	no effect	no effect
<i>Su(var)3-9</i>	<i>CG43664</i>	<i>Su(var)3-9⁶</i>			no effect	no effect
<i>Su(var)3-9</i>	<i>CG43664</i>	<i>Su(var)3-9¹³</i>			no effect	no effect
<i>Su(var)3-9</i>	<i>CG43664</i>	<i>Su(var)3-9²²</i>			no effect	no effect
<i>AGO2</i>	<i>CG7439</i>	<i>AGO2⁴¹⁴</i>	<i>Delta2-3 hypomorphic</i>	Argonaute 2 is essential for RNA interference (RNAi), bind to chromatin, possibly participates in insulator functioning	enhancement	weak enhancement
<i>AGO2</i>	<i>CG7439</i>	<i>AGO2^{51b}</i>	<i>Delta2-3 hypomorphic</i>		enhancement	weak enhancement

		Log2(A4/A12)					
Position	Gene	shH2MedKd	S2	shP2	S2	Insertion	Primer pair
21170816	<i>Acan</i>	-0.55	0.09	0.27	0.15	20708	+++ 20708rt
212164465	<i>CG6678</i>	-0.45	0.20	0.59	0.15	10879	+++ 10879_r12ex
212172715	<i>CG6679</i>	-0.70	0.12	1.07	0.03	10879	+++ 10879_r12_intragen
21237724	<i>10-29</i>	-0.12	0.11	1.40	0.16	55A12	+++ EP24905spAapr
213108055	<i>erc</i>	-0.19	0.38	1.04	0.14	12400	++ 12400rt

Primers for trans-inactivated region												Comments
Primer pair	Gene	Chr	Start	End	ID	Sequence	Start	End	ID	Antisense primer	Sequence	
19930Spr-19930A_Spr	CG9257	chr2L	21102549	21102578	19930Spr	CAATTCAATAAATAAAGAACGACGCA	21102746	21102781	19930A_Spr	CGGAATAATCATTTACAACTGATAGAATA		
19930_r1_s-19930_r1_as	CG9257	chr2L	21102753	21102782	19930_r1_s	ATACGAGTTTGTAATGGAATTTATCTCCG	21103054	21103079	19930_r1_as	CGGTTGACCGGATATAATACCTTCA		
20292Spr-1-20292A_Spr_1	Nhe2	chr2L	21108472	21108504	20292Spr_1	TAGACCATCTCTATATTTTACGTCTTCCAC	21108668	21108700	20292A_Spr_1	CCAGCAACAATTACAATATTTTCTATGTAGG		
19582Spr-19582_r1_as	Dup160	chr2L	21141834	21141860	19582Spr	TTATGTCCTCTTTCTATATGCTGTGT	21141976	21142001	19582_r1_as	AAATCAATTGTGAAATTTGTGGGG		
19661_r1_s-19661_r1_as	Dmwh24	chr2L	21143250	21143285	19661_r1_s	TGGTAAATTCCTGGTACCGTGAATTTT	21143426	21143453	19661_r1_as	CTTTATCATCTCACTACTAGTGTCCG		
deadlockSP-deadlockSP	deadlock	chr2L	21145570	21145598	deadlockASP	CAAAATTTCTGAGCAGTCTACGAGGA	21145728	21145753	deadlockASP	TGCCATCGAAGCTCACAAATATCG		
18010Spr-18010A_Spr	deadlock	chr2L	21147369	21147392	18010Spr	GAAGCGGGCAGTTGGTATCATAGA	21147560	21147587	18010A_Spr	GTGGTTCAGAGCGCAAGTACAAAGCT		
17314_r1_s-17314_r1_as	dlE2F2	chr2L	21152795	21152777	17314_r1_s	GATGATCATCTTGTTGGCTTCT	21152937	21152959	17314_r1_as	GATTCGGCTGAGACTCGGTCC		
5329_r1_s-5329_r1_as	Mup1	chr2L	21156881	21156910	5329_r1_s	GAAMAAATAAATGTCCTGATGGTTTC	21157094	21157121	5329_r1_as	TGGAAATGAGACTCTCTGGTGTGATCT		
16587_r1_s-16587_r1_as	Nbr	chr2L	21162710	21162730	16587_r1_s	TCAGGGCAGGAGCAAGAAGA	21162902	21162925	16587_r1_as	GAGCAACTGAAGTCAAGCGCTT		
ep2348_r1_s-ep2348_r1_as	CG9246	chr2L	21163629	21163650	ep2348_r1_s	CCGGTTGCAACGACACAGCTGC	21163811	21163832	ep2348_r1_as	GGCGGACTCTTCTGCTGGGT		
20708_r1_s-20708_r1_as	Acon	chr2L	21168651	21168681	20708_r1_s	TTTAGTCTCTCTTAAATCTTCCGGCTGAG	21168768	21168790	20708_r1_as	TCATCAATCTCGAGCAGCATGGT		
20708_2ndex_s-20708_2ndex_as	Acon	chr2L	21179486	21179513	20708_2ndex_s	ACAGATGGCTCTGCTGATGTTATCTC	21179538	21179563	20708_2ndex_as	AATGATCAAGTGAACGTGGAGGG		
20250Spr-20250A_Spr	bur	chr2L	21179461	21179486	20250Spr	GTTTCTCTCTCAGGCACACATCT	21179649	21179673	20250A_Spr	GGTCACTCCGCTCCTCAATAGTCA		
SP1171-ASP1936	Ret	chr2L	21185224	21185256	SP1171	TCTAGGGGATCACAGACATGATCTGGACAGTAA	21185392	21185422	ASP1936	GGCAACTGAAGGTCAAGTCTCGATCACAGAC		
20229Spr-20229A_Spr	Atg18b	chr2L	21205620	21205642	20229Spr	ACCCTGGATGACCAAGAACTGT	21205810	21205838	20229A_Spr	GACAAATCATACCTCTGAAACCAATGC		
10879_r1_2ex_s-10879_r1_2ex_as	Atg18b	chr2L	21214006	21214027	10879_r1_2ex_s	CTCTCACTGGCGAGAGAGACA	21214140	21214158	10879_r1_2ex_as	TTTCTCGCCAGCGGAG		
10879_r1_intgen_s-10879_r1_intgen_as	dlEM3	chr2L	21216329	21216351	10879_r1_intgen_s	AACCTGTATCTCCCTCCGCCA	21216454	21216478	10879_r1_intgen_as	GCCTCGGCTGTAATCACTTACC		
ep838_r1_s-ep838_r1_as	dlrf-1	chr2L	21221629	21221649	ep838_r1_s	AAGGACGACGACGCCCTCATC	21222493	21222515	ep838_r1_as	GGCGGACTCCCACTCTTTTTCG		
20152Spr-20152A_Spr	H939	chr2L	21237113	21237135	20152Spr	AGTAAACCAAGCTCGTGGCTCT	21237299	21237322	20152A_Spr	AATCGGATCCCAACCGCTCTA		
EP240Spr-EP240A_Spr	H939	chr2L	21237724	21237747	EP240Spr	TGCGTGTGATGACCCCTTACC	21237915	21237940	EP240A_Spr	GCCTCTTGTTGGTTTCCCACCTT		
H939_r1_s-H939_r1_as	H939	chr2L	21238409	21238439	H939_r1_s	AATGTCACTAGAATGTGATCGCAACAACAC	21235591	21235620	H939_r1_as	TTCTCACTGTGCTAATTTGTAAGTTTG		
EP250Spr-EP250A_Spr	H939	chr2L	21250772	21250796	EP250Spr	AACCCCAAAAAGATGACGACAGC	21250956	21250980	EP250A_Spr	CCAACCAACACCATGAGGACAGCA		
11127_r1_s-11127_r1_as	E2H14505	chr2L	21261169	21261198	11127_r1_s	CACGTAAACCTCACTCTGCTTAAACA	21261266	21261289	11127_r1_as	TGAATTTGGTCAACCCGAGAGCT		
11015_r1_s-11015_r1_as	CG8671	chr2L	21262980	21263013	11015_r1_s	GCATCATCGGTGATCTGCTGTGC	21263055	21263078	11015_r1_as	GCCTATACACTTCCGACAGAA		
11015Spr_3-11015ASpr_3	CG8671	chr2L	21263232	21263257	11015Spr_3	GAGGACATACATTTTCCAGTCGCTT	21263405	21263434	11015ASpr_3	CGAGATGTTTATATTCACACACAGCTTT		
20102Spr_2-20102ASpr_2	Mlo	chr2L	21309657	21309682	20102Spr_2	CAGATGTGAGGCAAGATGTTGCTC	21309861	21309887	20102ASpr_2	GGTCACTGAGTTGTACCGAAATGTG		
12400_r1_s-12400_r1_as	erc	chr2L	21310855	21310881	12400_r1_s	TGATCTCAACACTATCATCGTCCA	21310922	21310952	12400_r1_as	GGCATCTTTAGGTAAATATAAATGCGGAA		
CG8665_2ex_s-CG8665_2ex_R	CG8665	chr2L	21374324	21374343	CG8665_2ex_s	GGGCTACATAGATGTTGTTG	21374413	21374432	CG8665_2ex_R	TGAGCTGGGAGGATAGAGAG		
nompB_Alex-nompB_Alex_R	nompB	chr2L	21585667	21585856	nompB_Alex_F	TTACAGTTACCGCCACTCT	21586733	21586753	nompB_Alex_R	TTCGAGAGCTTTGTGATCTCC		
CG2201_F-CG2201_R	CG2201	chr2L	21615144	21615163	CG2201_F	ACCAAGGCTCCAGAACAGA	21615302	21615322	CG2201_R	CTTCTACCAACCTCAGGAA		
DF31	DF31	chr2L	21628069	21628092	10579_r1_s	CTCTGGTACGCTCTCTCTCTTCG	21629721	21629742	10579_r1_as	CGTGTTTTCTCGCTCGCTGT		
CG2225_F-CG2225_R	CG2225	chr2L	21766897	21766916	CG2225_F	AAATCTAGCAGCGCTTTC	21766993	21766912	CG2225_R	CTTTTGGCTGGTGAACCTT		
10770_r1_s-10770_r1_as	step	chr2L	21756571	21756591	10770_r1_s	TTCTGCTCTCTGGTGCGCA	21757187	21757212	10770_r1_as	AGATCGTACGCTGCCATCAAAGG		
10770Spr-10770A_Spr	step	chr2L	21756671	21756698	10770Spr	TTCTGGGCAATTTGTAAATGTATGTC	21756848	21756873	10770A_Spr	AGCATCATTTGTGTTTGCAGAC		
Other used primers												
60Dw-60Dw	chr2R		20322298	20322317	60Dw	TTCCCATCTCTCGAGCCCTG	20322447	20322469	60Dw	CCAGCCGAGACGAGCACCATAAT		Used for sample quantity normalisation in ChIP experiments
Rp49v-Rp49v-2	Rp432	chr3R	25871481	25871501	Rp49v	ATGACCATCTCCGCCACATAC	25871414	25871436	Rp49v-2	GCTTACATATCATCGCAGCTGG		Used for sample quantity normalisation in RT-qPCR experiments
Hs1 coding s1-Hs1 coding as1	white	chrX	2687189	2687216	Hs1 coding s1	CGTCCGCTCTCCCGAGTG			Hs1 coding as1	CTTGAGCGATTTCAGCGACCA		Used for synthesis of fluorescent probe to histone genes cluster
miniwh1_int_s-miniwh1_int_as	LacZ				miniwh1_int_s	AACCTAAGCGTTATGCTCATTAACC	2689961	2690063	miniwh1_int_as	CTTAAGGCGATTCAATTTGCGATCAATCT		Probe for mini-white gene in ChIP experiments
DSG3-DSG4					DSG3	TTCTATGTCGGTGGTGACCTA			DSG4	CGCGATGGTTCGGATAATGC		Probe for LacZ gene in ChIP experiments
					Biot-AACAC	Biot-(A)CAGC						Biotilated probes for satellite DNA
					Biot-AATAACATAG	Biot-(A)ATAACATAG)S						Biotilated probes for satellite DNA
	chr2L		21150730	21150759	S39C1150540	AAACAATCAAACTCCGAGAAAGCAAGCA						Primers used for A4 breakpoint mapping and probe synthesis
	chr2L		21150851	21150880	AS39C8049	AAAGCAAGATGACCGAGCAACAAATGG						Primers used for A4 breakpoint mapping and probe synthesis
	chr2L		21158849	21158878	S39C96254	GACTGTGACGAGCAACCAATGAGTGGAG						Primers used for A4 breakpoint mapping and probe synthesis
	chr2L		21166230	21166253	AS39C1150540	GAAGAAGCAAGCGCGCGCAATG						Primers used for A4 breakpoint mapping and probe synthesis
	chr2L		21167355	21167383	S8939C1419	CGCGTCTCTTTGATTTGATGTCGGTGTG						Primers used for A4 breakpoint mapping and probe synthesis
	chr2L		21173423	21173453	AS39C5453	AAGTGTAGAGAGCTGTGCTGAGTCAAGG						Primers used for A4 breakpoint mapping and probe synthesis
	chr2L		21176947	21176971	S8939C11116	ACGGACTGTGTGCTGACGAGGAGCA						Primers used for A4 breakpoint mapping and probe synthesis
	chr2L		21181387	21181416	S39C1181389	CTAACCAACCTCAAACTCCCAAAACAGCC						Primers used for A4 breakpoint mapping and probe synthesis
	chr2L		21181387	21181416	ASBP93C1419	GGCTGTTTGGGGCTTTGAGGTGTGGTTAG						Primers used for A4 breakpoint mapping and probe synthesis
	chr2L		21183463	21183488	AS39C1181389	CAACGGCGAGCTTTTGCTGATACGA						Primers used for A4 breakpoint mapping and probe synthesis
	chr2L		21183486	21183511	S8939C17560	TGGCGGTAGCATCAACGAAAGTCTG						Primers used for A4 breakpoint mapping and probe synthesis
	chr2L		21187542	21187572	ASBP93C18124	GCACGGGAATAGAAACGGGAACCAAGTG						Primers used for A4 breakpoint mapping and probe synthesis
	chr2L		21187736	21187764	S39C98487	CGTGGTAAATAGCGTCTGCGAGGAAGC						Primers used for A4 breakpoint mapping and probe synthesis
	chr2L		21196811	21196845	S39C1196813	AGACACGAGAGCGCATCACTACGATGACTG						Primers used for A4 breakpoint mapping and probe synthesis
	chr2L		21196811	21196845	ASBP93C17560	CAGTCACTGAGTCAATGCTGCTGCTCTGCTCT						Primers used for A4 breakpoint mapping and probe synthesis
	chr2L		21199728	21199752	S39C1202044	TTGCAGCGCGCACAGGTGATGTTG						Primers used for A4 breakpoint mapping and probe synthesis
	chr2L		21203030	21203060	S39C91019	GGGAGGCTCTCACTTCAATGGGTGATTTCT						Primers used for A4 breakpoint mapping and probe synthesis
	chr2L		21203993	21204017	ASBP93C1204735	CACAGATCTGCTGCTCCACCGAGTG						Primers used for A4 breakpoint mapping and probe synthesis
	chr2L		21204167	21204194	AS39C1204815	CGCTGACACAATTCCTACCTCGATCT						Primers used for A4 breakpoint mapping and probe synthesis
	chr2L		21210234	21210262	4_inversion region a	CGCGAGGATCTGCTGCGCAACCAATAA						Primers used for A4 breakpoint mapping and probe synthesis
	chr2L		21210992	21211018	AS39C1196813	TGAAGCAAGCGGAGCAAGCAACCA						Primers used for A4 breakpoint mapping and probe synthesis
	chr2L		21218750	21218780	4_inversion_region_a	GCACACAGTGTGTTGTTATTTCTTGACT						Primers used for A4 breakpoint mapping and probe synthesis
	chr2L		21218847	21218876	4_inversion_region_a	CTCAATGCGCTATGCTACAAAGGGGTA						Primers used for A4 breakpoint mapping and probe synthesis
	chr2L		21226988	21227015	4_inversion region a	GGCAGTCCGCAAGGCTCAAAAGGTAA						Primers used for A4 breakpoint mapping and probe synthesis
	chr2L		21227005	21227028	4_inversion region a	TCGCGGAGCGCGTTTACCTTT						Primers used for A4 breakpoint mapping and probe synthesis
	chr2L		21235104	21235125	4_inversion region a	CAGAGCGCGGGTGAGGGCTCG						Primers used for A4 breakpoint mapping and probe synthesis
	chr2L		21235108	21235112	4_inversion region a	CCTCACTCCGGCTCTGCTTATTG						Primers used for A4 breakpoint mapping and probe synthesis
	chr2L		21244072	21244100	4_inversion_region_a	ACTGTCTTGGTGGCTGCTGGCTCTCG						Primers used for A4 breakpoint mapping and probe synthesis
	chr2L		21244079	21244109	4_inversion_region_a	GCCAGAGCGCCACCAAGATGAACACAG						Primers used for A4 breakpoint mapping and probe synthesis
	chr2L		21251826	21251850	4_inversion region a	GGAGCGGCGAGGATCAATGAGCAAT						Primers used for A4 breakpoint mapping and probe synthesis
	chr2L		21251838	21251858	4_inversion region a	CTCCGCGCTGATGCTGCG						Primers used for A4 breakpoint mapping and probe synthesis
	chr2L		21260077	21260106	4_inversion region a	CGCCATTCTATGCGCTAAAGCTGGAA						Primers used for A4 breakpoint mapping and probe synthesis
	chr2L		21210832	21210858	S39C71	ATCAGTGGCGGAGTGTCAAGTTGGG						Primers used for A4 breakpoint mapping and probe synthesis
	chr2L		21218352	21218379	AS39C71	CCCTGGAGGAGGAGCAAGGAGCTGATA						Primers used for A4 breakpoint mapping and probe synthesis